

COFFEE ROASTING PROCESS MONITORING WITH *IN SITU* NIR
SPECTROSCOPY

A Thesis

Presented in Partial Fulfilment of the Requirements for the
Degree of Master of Science

with a

Major in Chemical Engineering

in the

College of Graduate Studies

University of Idaho

by

Nathan Yergenson

Major Professor: Eric Aston, Ph.D.

Committee Members: David Drown, Ph.D.; Brennan Smith, Ph.D.

Department Administrator: Eric Aston, Ph.D.

May 2019

Authorization to Submit Thesis

This thesis of Nathan Yergenson, submitted for the degree of Master of Science with a major in Chemical Engineering and titled "Coffee Roasting Process Monitoring with *In Situ* NIR Spectroscopy," has been reviewed in final form. Permission, as indicated by the signatures and dates given below, is now granted to submit final copies to the College of Graduate Studies for approval.

Major Professor: _____ Date _____
Eric Aston, Ph.D.

Committee
Members: _____ Date _____
David Drown, Ph.D.

_____ Date _____
Brennan Smith, Ph.D.

Department
Administrator: _____ Date _____
Eric Aston, Ph.D.

Abstract

There is a need in the roasting industry for better real time feedback during roasting to consistently achieve the desired qualities in roasted coffee, and NIR spectroscopy has shown some promise for this purpose.

This project generated a new roast degree scale based on *in situ* NIR prediction of the cracking sounds which are commonly used as a real time indication of roast degree. This required measuring the start and end times of the two crack events by analyzing recorded audio from a large set of roasts including eight varieties of coffee with four roast temperature profiles each. An NIR spectrometer with a custom diffuse reflectance probe attached to the roaster recorded *in situ* spectra during each roast for predicting the crack event times and determining the roast degree.

Measurements of coffee acidity provided a basis for comparing the newly developed crack scale to two other scales: a simple scale generated based on NIR absorbance and the common CIELAB scale based on visible color. Both NIR based scales performed better than the visible scale in this comparison, and the simple NIR scale performed best. This scale was then used as a basis for determining the effects of different roast temperatures on acidity, to explore the ability to control acidity independent of roast degree. A new set of constant temperature roasts provided the dataset for this analysis, resulting in simple linear relationships between roast degree, roast time, and acidity.

Acknowledgments

First, I would like to thank my major professor Dr. Eric Aston for making this project possible and for his guidance and endless supply of curiosity and interest. I would also like to thank my committee members, Dr. Dave Drown and Dr. Brennan Smith, for their sound advice and time, and Charles Cornwall and Dr. Dave MacPherson for their assistance in designing, fabricating, and automating the equipment used in this project. Finally, I am grateful for my family and Qiuping Peng for all of their support throughout this process.

Table of Contents

Authorization to Submit Thesis	ii
Abstract	iii
Acknowledgments	iv
Table of Contents	v
List of Figures	viii
List of Tables	xi
1 Introduction and Background	1
1.1 Coffee Production Background	1
1.2 Roast Degree Measurement	5
1.2.1 Industry Methods	5
1.2.2 NIR Roast Degree Measurement	6
1.3 Coffee Chemistry and Flavor	10
1.3.1 Controlling Coffee Flavors with the Roasting Temperature Profile	12
1.4 Objectives	14
2 Monitoring Coffee Roasting Cracks and Predicting with <i>in Situ</i> NIR Spec-	
troscopy	16
2.1 Abstract	16
2.2 Introduction	16
2.3 Methods	18
2.3.1 Coffee Roasting	18
2.3.2 Crack Detection	19
2.3.3 <i>In Situ</i> NIR	20
2.3.4 NIR Data Analysis	21
2.4 Results and Discussion	22

2.4.1	Sound Analysis	22
2.4.2	NIR Spectra	24
2.4.3	PLS Models for Crack Prediction	26
2.4.4	Numeric Roast Degree Scale	29
2.5	Conclusions	30
3	Online Determination of Coffee Roast Degree toward Controlling Acidity	31
3.1	Abstract	31
3.2	Introduction	31
3.3	Methods	33
3.3.1	Roasting and Sampling	33
3.3.2	<i>In Situ</i> NIR	33
3.3.3	Ground NIR	34
3.3.4	Lightness Measurement	34
3.3.5	Titrateable Acidity	34
3.4	Results and Discussion	34
3.4.1	NIR Roast Degree	34
3.4.2	Comparing NIR Darkness to Visible Lightness	36
3.4.3	Comparing Online and Ground NIR Darkness	37
3.4.4	Titrateable Acidity Results	38
3.4.5	Roast Scale Comparison	39
3.4.6	Acidity Control Roast Profiles	42
3.4.7	Acidity Control Roast Results	42
3.5	Conclusion	46
4	Conclusion and Recommendations	47
	References	50
A	Roast Degree Acidity Data	56
B	Crack Data	60
C	Crack PLS Coefficients	62
D	Scaled Acidity Plots	63
E	Acidity Control Data	65

F	Coffee Body Measurement Attempts	67
	F.1 Contact Angle	67
	F.2 Viscosity	70
G	Predicting Acidity with PLS Regression	71
H	Full Range NIR Spectrum	73
I	Online NIR Validation	75
J	Crack Roast Degree Example	77

List of Figures

1.1	Coffee beans at different stages of roasting from left to right: unroasted, before first crack, after first crack, before second crack, after second crack.	3
2.1	Inlet air temperature-time profiles used in roasting	19
2.2	Schematic of the roaster with NIR mount	20
2.3	Fourier transform (left) and raw audio data from two first crack sounds (a-d) and two second crack sounds (e-h)	23
2.4	Histograms of first crack times from 12 roasts (a) and second crack times (b) from 5 roasts	24
2.5	Time-series-spectral-overlay after Savitzky-Golay filtering taken during a roast with the wavelengths used in the NIR darkness predictor ($7700\text{-}7142\text{ cm}^{-1}$ and $6667\text{-}6225\text{ cm}^{-1}$) highlighted. (a). The resulting NIR darkness value vs time throughout the roast (b).	25
2.6	MSC treated time-series-spectral-overlay with regions-of-interest labeled	25
2.7	NIR spectrum before cooling subtracted from the spectrum after 60 s of cooling comparing two light source intensities	26
2.8	Prediction plots of PLS models vs measured NIR darkness offset (AU) values. Values represent the change in NIR absorbance which will occur before the event of interest. A value of 0 occurs at the event, positive values before, and negative after. The four plots represent first crack start (a), first crack end (b), second crack start (c), and second crack end (d).	28
2.9	Roast degree predictions from <i>in situ</i> NIR compared to actual roast degree from crack times measured with a microphone	30
3.1	Mean NIR absorbance over three wavelength ranges: 1300-1400 nm (a), 1500-1600 nm (b), and 1900-2000 (c) and the absorbance resulting from subtracting two ranges: c-a (d) and b-a (e).	35
3.2	NIR darkness (a) and visible lightness (b) plotted against time for all eight coffee varieties roasted with profile 1.	36

3.3	Comparison of NIR darkness values measured online vs offline ground.	37
3.4	Comparing offline vs. ground NIR darkness correlation for high temperature fast roasts to low temperature slow roasts with separate trend lines (dotted).	38
3.5	Measured and scaled acidity values vs NIR darkness for one coffee variety (Kenya).	39
3.6	Comparing scaled titratable acidity values on three roast degree scales (columns 1-3), separated by roasting temperature profile (rows 1-4). Points from each roast are connected by lines representing eight coffee varieties.	40
3.7	Box plots showing the roast degree values at first crack start (FCS), first crack end (FCE), second crack start (SCS), and second crack end (SCE) for NIR darkness and visible lightness roast degree scales.	41
3.8	Outlet air temperatures (solid line) during the first 500 s of three constant inlet temperature roasts (dotted lines).	42
3.9	Constant temperature roast results for acidity control. Each line results from multiple roasts with the same coffee variety, to approximately the same NIR darkness roast degree, with different inlet air temperatures.	43
3.10	Residuals of the acidity model by time (a) and NIR darkness roast degree (b).	44
3.11	NIR darkness roast degree values observed in three example roasts (solid lines) with the modeled results (dotted lines).	45
3.12	Relationship between acidity, roast time, roast degree (shown by color), and temperature (white lines) based on regression models for acidity and roast degree.	46
4.1	Design of a simple NIR darkness sensor.	48
C.1	Absolute value of the PLS predictor importance in the models for first crack (a) and second crack (b) with the most important regions labeled A-F. Results have been smoothed to improve readability.	62
D.1	Acidity scaled by the maximum acidity measured. First 4 varieties.	63
D.2	Acidity scaled by the maximum acidity measured. Last 4 varieties.	64
F.1	Contact angle on Rain-X® coated slides on an aluminum block heated to 70 °C.	68

F.2	Contact angle on Rain-X® coated slides on an aluminum block heated to 70 °C with the brewed coffee kept in a boiling water bath.	68
F.3	Contact angle on InSnO coated slides on an aluminum block heated to 70 °C with the brewed coffee kept in a boiling water bath.	69
F.4	Rain-X® coated slides heated to 37 °C (a) and InSnO coated slides without heating (b). In both cases, the coffee was in a boiling water bath until removed for sampling.	69
G.1	Plot of acidity predictions vs measured values.	71
G.2	Plot of acidity predictions vs measured values for a set of roasts to the same final roast degree with different roast profiles.	72
H.1	Combined online NIR data from two NIR spectrometers with different wavelength ranges measured on two identical roasts.	73
I.1	NIR spectrum of the glass roasting chamber with a Teflon block inside, after subtracting the spectrum of the Teflon block without the roasting chamber as a reference.	75
I.2	NIR spectra of the empty glass roasting chamber at room temperature and at 230 °C.	76
J.1	Sample calculation of roast degree from crack predictions based on NIR darkness offset.	77

List of Tables

1.1	Summary of Articles using NIR to measure coffee roast degree. ⁽¹⁾ Standard Normal Variates, ⁽²⁾ Orthogonal Signal Correction, ⁽³⁾ Direct Orthogonal Signal Correction ⁽⁴⁾ Fourier Transform	8
2.1	List of coffee varieties used in this study	18
2.2	PLS regression results. The number of points for each model is different because of the selection criteria and includes both calibration and test data. ⁽¹⁾ Range Error Ratio	27
2.3	Reference numbers used in defining a roast degree scale based on the crack events. A roast ending between two events receives a roast degree between the two reference numbers. The exact value is determined by the output of the PLS models.	29
3.1	Results of linear regression fits on the three roast degree scales vs. acidity. Root mean square error (RMSE) values are in terms of unit-less scaled acidity.	41
A.1	Titrateable acidity results for 32 roasts with 4 samples per roast. Used for comparing roast degree scales and to generate a PLS model based on acidity.	56
B.1	Crack start and end times determined by recorded audio from 32 roasts with 8 coffee varieties and 4 roast temperature profiles.	60
E.1	Data from constant temperature roast profiles for acidity control described in Chapter 3	65
F.1	Coffee viscosity results	70

CHAPTER 1 Introduction and Background

Coffee is the world's most popular beverage besides water, with 9.4 million metric tons of green coffee beans produced in the 2016-17 growing season [35, 38]. The global average price for green coffee during this season was only \$1.32 per pound, but roasted coffee in stores commonly sells for more than \$5 per pound. Roasting is responsible for the majority of this increase, and consequently, the quality and consistency achieved through roasting are critical to the value of the final product. Unfortunately, methods of achieving this are lacking, and many roasters still rely on sensory perceptions to guide the roasting process, often resulting in inconsistency and requiring a lengthy trial-and-error process to determine the optimum parameters for roasting a new variety of coffee [48].

1.1 Coffee Production Background

Coffee production can be broken down into four steps, all of which can have a significant impact on the characteristics of the beverage. These steps are growth, processing, roasting, and brewing.

Plant variety is the most important factor related to coffee growth. There are four species of coffee on the market today (arabica, robusta, liberica, and excelsa), although only arabica and robusta are widely traded [38]. The flavor and aroma of arabica coffee are generally considered to be superior, and arabica makes up 60-70% of world production. There are numerous varieties of arabica and robusta on the market as well, and new varieties are being bred with the primary purposes of increasing disease resistance and productivity [3]. Soil and climate also play an important role in the quality of the final beverage, and coffees produced in acidic soil and at high elevations are generally considered superior. Growth is restricted to lower latitudes, as the plants cannot survive freezing. Coffee plants develop a fruit, called a coffee cherry, inside of which are two seeds. Although commonly referred to as coffee beans, they are technically not beans.

After harvesting, the seeds must be removed from the coffee cherry and dried.

There are several methods for this processing step which have a considerable impact on the final product [8, 48]. The simplest method is referred to as natural or dry processing and consists of sun drying the cherries on patios and breaking the dried fruit off the seed. The prolonged contact with the fruit in this method results in more fruity aroma in the final product, but lower acidity and often lower cup scores, a rating resulting from a standardized tasting procedure, than the other methods. Alternatively, machines can remove the outer skin from the cherry, leaving some of the pulp still attached. Coffee that is dried naturally on patios at this point before removing the remaining pulp is called pulped natural or honey processed. Because the drying is quicker than the natural method, the resulting coffee has higher acidity and less fruity aroma. Instead of allowing the pulped coffee beans to dry, the pulp can also be removed by fermenting the coffee in tanks for 8 to 72 hours [56] after which it will easily be removed. This is referred to as washed or wet processing, and since the coffee spends less time in contact with the fruit, the resulting coffee has higher acidity than the first two methods. Due to higher cup scores, the fast turnaround time, and still relatively low equipment costs, wet processing is the most common [8]. All three of the above methods involve some time where the coffee is influenced upon by microbes, either during intentional fermentation steps to remove the pulp or while the coffee is naturally drying. Instead of allowing wild yeast to perform this step, inoculating with different strains of yeast has become a promising new area of interest, which may have the ability to produce new aromas [27, 41, 50, 56]. An alternative to fermentation in the wet processing method is mechanically removing the skin and pulp in a single machine, which is referred to as mechanical demucilagination and minimizes the opportunity for microbes to act on the coffee. Additional steps that take place before the coffee is exported are cleaning, hulling, polishing, sorting, and storage [8].

The third step in the coffee production process is roasting. Roasting is responsible for generating the characteristic flavor and aroma and coffee and accomplishes this in a very short time-frame. Typical roasts last 7 to 20 minutes, although coffee has been roasted in as little as one minute in fast roasting conditions, which increases the yield of soluble mass at the expense of homogeneity and perceived quality [10]. After the start of roasting the temperature rises until the beans begin to turn yellow. This is the first visible change and is considered the start of the “drying phase.” Soon after, the beans begin to turn brown, which is attributed to the Maillard reaction, the non-enzymatic browning reaction which also causes the browning of bread crust [59]. Near this time, chlorogenic acids from the green coffee begin to break down, and by the time the coffee reaches a light roast, the coffee loses more than half of its chloro-

genic acid content [42]. As the roast continues, the coffee begins to pop, sounding similar to popcorn, in an event called first crack. Heat and mass transfer models of coffee roasting predict the formation of a sharp drying front in the bean, outside of which there is no liquid phase water, which moves toward the center of the bean [28]. As it approaches the center, the pressure gradient increases, which may eventually overcome the strength of the bean, causing the center to burst. The cavity caused by the first crack can be seen in Figure 1.1. The end of first crack is often considered the start of a light roast.



Figure 1.1: Coffee beans at different stages of roasting from left to right: unroasted, before first crack, after first crack, before second crack, after second crack.

After first crack, the coffee continues to darken gradually, and the transition point to a medium roast has no clear indication. The Maillard reaction continues, and caramelization and pyrolysis begin to occur as the temperature increases. Eventually, the coffee begins to emit another set of cracking sounds, called second crack, which marks the transition to a dark roast. Second crack is associated with the release of oils to the surface of the bean, and while the cause of second crack remains uncertain, suggested possibilities include CO_2 pressure or fracturing of the cell matrix [48, 61]. Coffee roasted to the end of the second crack is typically considered burnt, and even dark roasts typically end somewhere in the middle of the event [22, 48].

During roasting, the physical properties of the coffee change drastically [10]. The

beans lose the majority of their moisture content and 5-8% of their organic mass in a medium to dark roast while increasing in volume due to internal pressures estimated in excess of 15 atm [28]. This causes a typical change in density of 70%.

The final process before coffee can be consumed is grinding and brewing. Two parameters often used to describe the result of the brewing process are concentration and level of extraction [31]. Concentration is the strength of the beverage, measured as percent total dissolved solids (TDS), and extraction is the fraction of total soluble material extracted from the coffee. While the preferred strength varies with brewing method, the optimum extraction range is always 18-22% for brewed coffee and espresso [11]. If the extraction is too low, the beverage will contain a higher fraction of the most soluble components which dissolve most quickly (*e.g.* acids), making the coffee taste under-developed or sour. If the extraction is too high, some undesirable components with lower solubility begin to reach noticeable levels, causing the coffee to taste bitter and astringent.

The ability to choose a grind size and to grind the coffee consistently and uniformly is important to achieve the desired extraction level and strength, especially in brew methods where grind size influences brew time, such as espresso and drip. Coffee grinders can be split into two categories: impact grinders and gap grinders [45]. Impact grinders consist of rotating blades that exert a shock on particles in their trajectory, causing them to break. The particles remain in the path of the blades no matter how small, so these grinders are not good at regulating size. Gap grinders consist of two cutters (or burrs) with a gap between them, which move relative to each other. Particles pass through the gap after being cut, so the size of the gap determines the size distribution.

Many different brew methods have been developed in coffee's long history, but they can be split into three categories: decoction, infusion, and pressure methods [19]. Decoction methods involve adding the coffee to the water before it is brought to boiling (*e.g.* percolators and Turkish coffee), infusion methods involve heating the water before adding the coffee (*e.g.* pour-over or auto-drip coffee), and pressure methods use high pressure to push the water through the coffee, as with espresso. An additional important factor is the use of a paper filter, which eliminates sediment, but can remove oils and small particles, which contribute to the flavor and body.

1.2 Roast Degree Measurement

1.2.1 Industry Methods

Roast degree may be the most important metric describing coffee roasting, because the flavor of the same coffee changes drastically when roasted to different degrees. Light roasts are often acidic and bring out the unique characteristics of the variety of coffee being roasted. Medium roasts have lower acidity and more body than light roasts, making them the mildest roast and allowing the sweetness of the coffee to be more easily perceived. Dark roasts take on new smoky and roasted aromas, the highest level of body, and often increased bitterness relative to the other roasts. Differences in water content, size, and chemical composition can cause different coffees to roast differently, even when the same temperature-time roasting profile is applied, making the ability to measure roast degree in real time necessary.

Color is the roast degree indicator most familiar to coffee consumers, but changes in color can be difficult to judge visually and may be perceived differently depending on the observer or the lighting. To help with this, there are colorimetric roast analyzers, which can measure the color of the coffee based on the CIELAB color scale [36]. This scale breaks color into Luminance/Lightness (L^*), a red-green value (a^*), and a yellow-blue value (b^*). The asterisks are used to separate the current CIE version of the color scale from an older version. These roast analyzers take the subjectivity out of measuring roast color, but there is still some question as to whether color is an acceptable measurement of roast degree.

The color of roasted coffee can be affected by a variety of factors not related to roast degree. It is apparent when looking at different green coffee varieties that the initial color of the green coffee can vary, but different coffee varieties are also known to change color at different rates during roasting. The rate of color change is affected by the processing method of the green coffee, as coffee processed with the natural method require a higher temperature to reach the same color as coffees processed with the washed method [10]. Even the temperature profile followed during roasting can affect the final color of the roasted coffee. One study compared CIELAB color to roast loss, the percent reduction in dry mass of the coffee, after roasting with different temperature profiles and found that the relationship between color and roast loss differs for different temperature profiles [46]. These observations all indicate that color is not a suitable property for determining roast degree.

The first and second crack events are commonly used as references for roast de-

gree, with the end of the first crack typically representing a light roast and the start of the second crack marking the transition from a medium to a dark roast. This does not provide any information about roasts between these two levels. For example, a full city roast, the most popular roast point in the US, can be described as ending “just before the start of second crack,” but this is difficult to judge without knowing when second crack will start. For this method to be more useful, the ability to predict the start of second crack and an actual measurement of the progression between first crack and second would be useful. This is one area where online NIR spectroscopy may be able to add value to the roasting process by providing such a prediction.

The percent mass loss during roasting is also sometimes used as a measure of roast degree, but it cannot easily be measured in real time. Roasting loss is the loss in dry mass, after subtracting the change in water mass, which provides an indication of the cumulative chemical changes [10]. This may be another area where NIR predictions could prove useful by making roast loss predictions available in real time.

1.2.2 NIR Roast Degree Measurement

Near-infrared (NIR) is the region of light from 800 to 2500 nm or 12,500 to 4000 cm^{-1} [43]. Diffuse reflectance measurements in this region primarily yield information about the overtones and combinations of vibrations which have fundamental frequencies in the infrared region. The most prominent signals are caused by overtones and stretching-bending combinations of OH, NH, CH, and SH bonds. This makes NIR spectroscopy useful in the identification of many organic compounds, but because of wide peaks which overlap heavily, determining the chemicals responsible for individual peaks is often not possible. Instead it is necessary to resort to chemometrics to extract information from NIR with techniques like principle component analysis (PCA) and partial least squares (PLS) regression.

The ability to use optical fiber probes in non-destructive analysis has made NIR spectroscopy a technique of interest in many applications, including coffee. Applications for NIR with coffee include determination of defects and adulterants, measurement of caffeine content, prediction of sensory properties, and measurement of roast degree [7]. Multiple studies have focused on the measurement of roast degree with NIR and most have used the prediction of color as the primary metric (Table 1.1). The first such study [25] achieved a determination coefficient (R^2) of 0.925 using PLS regression to correlate the NIR spectra to color measured with a visible spectrometer. This is a low R^2 value relative to the three other characteristics measured in the

same study, which were total acidity, caffeine content, and chlorogenic acid content. The authors suggest this is because color is a visible quality and the NIR wavelength range reflects chemical properties. Although it is not considered a chemical property, the color of coffee follows a darkening trend with increasing roast degree, which can be related to changes in the chemistry of the roasting coffee and allows color to be indirectly predicted by NIR. Given the unsatisfactory ability of NIR to predict color, the amount of emphasis placed on it is unsubstantiated, especially considering that visible spectrometers, which can directly and accurately measure color, are generally less expensive than NIR spectrometers. Bertone et al. [9] used a modified version of the PLS algorithm to measure color and arabica/robusta content simultaneously with an R^2 value of 0.87. This is an even further reduced accuracy than the first study, possibly because of differences in the regression method, pre-processing methods, or the fact that blends of arabica and robusta coffee varieties were used instead of single variety samples. Santos, Viegas, et al. [53] used NIR to predict color *in situ* with an R^2 of 0.94.

The remaining study used NIR to measure roast degree based on density, weight loss, and moisture content with R^2 values of 0.986, 0.954, and 0.977, respectively [2]. Except for moisture content, these properties are also not direct measurements of chemical properties, but the quality of the fits suggest that they are strongly correlated with chemical changes in the coffee, allowing them to be predicted with NIR.

It is useful to look at the methodology these studies used to collect and treat data for regression as this has a significant impact on the quality of the regressions. The first step in implementing PLS regression is to collect a large set of data by roasting different coffees with multiple roasting times and temperatures, taking the NIR spectrum of each roast, and measuring the properties to be correlated. The number of roasted coffee samples collected for the data set ranged from 52 to 168 in these four studies. This data set is then often split into two subsets for regression. The calibration set is used to produce the model and typically comprises 75 to 80 percent of the data, and the prediction set is used to test the model.

The NIR spectrometers varied for each study, and the wavelength ranges they measured were all slightly different. Four of the five used Fourier Transform (FT) NIR spectrometers and only one used a standard grating spectrometer. All four studies used extended wavelength NIR spectrometers with a high-end wavelength between 2200 and 2857 nm as opposed to the limit of approximately 1700 nm reached by spectrometers without the extended range, and this extended range does appear to contain information which is important for identifying characteristics of coffee based

Table 1.1: Summary of Articles using NIR to measure coffee roast degree. ⁽¹⁾Standard Normal Variates, ⁽²⁾Orthogonal Signal Correction, ⁽³⁾Direct Orthogonal Signal Correction ⁽⁴⁾Fourier Transform

Title	Published	Attributes Measured-R ²	Samples	Wavelength Range Measured (nm)	Pre-Processing	Regression Method
Prediction of roasting colour and other quality parameters of roasted coffee samples by near infrared spectroscopy. A feasibility study [25]	2004	Acidity-0.987 Chlorogenic Acids-0.957 Caffeine-0.998 Color-0.925	83 (4 arabica and 5 robusta varieties)	1100-2200	Mean Centered, First Derivative, SNV ⁽¹⁾ , OSC ⁽²⁾ , DOSC ⁽³⁾	PLS
Near infrared spectroscopy: An analytical tool to predict coffee roasting degree [2]	2008	Density-0.986 Weight Loss-0.954 Moisture Content-0.977	168 (4 arabica, 2 robusta, 2 blends)	830-2500 (FT ⁽⁴⁾)	Vector Normalization, First Derivative, Second Derivative	PLS
Simultaneous determination by NIR spectroscopy of the roasting degree and Arabica/Robusta ratio in roasted and ground coffee [9]	2016	Color-0.87 Arabica/Robusta Ratio-0.97	130 (Blends of arabica and robusta)	800-2857 (FT)	First Derivative	PLS2 (multiple outputs)
Exploiting near infrared spectroscopy as an analytical tool for on-line monitoring of acidity during coffee roasting [52]	2016	Acidity-0.89	52 (2 arabica and 2 robusta varieties)	1000-2500 (FT)	Mean Centered	PLS
In-line monitoring of the coffee roasting process with near infrared spectroscopy: Measurement of sucrose and colour [53]	2016	Sucrose-0.93 Color-0.94	52 (2 arabica and 2 robusta varieties)	1000-2500 (FT)	SNV, First Derivative, Second Derivative	PLS

on these studies.

Several methods are available for pre-processing of the NIR spectra before regression, and the pre-processing method appears to have a substantial impact on the accuracy and robustness of the resulting model. Pre-processing methods improve the regression results either by removing noise (filtering), correcting for baseline shift, or modifying the NIR spectra in some other way to improve the results of the regression algorithm [43]. One of the groups correlating coffee color and some three other characteristics to NIR [25] considered the impact of several different pre-processing methods on the results. They compared PLS regression results after pre-processing with mean-centering, standard normal variate (SNV), first derivative, orthogonal signal correction (OSC), and direct orthogonal signal correction (DOSC), and used the percent of variance explained by the PLS regression in the calibration set and prediction set as metrics to compare the different methods. The percent of explained variance for both sets should be as high as possible, but if the percent of explained variance for the validation set is significantly higher than for the prediction set, it is a sign of overfitting. In the regressions performed by Esteban-Diez et. al., the results with OSC and DOSC were best. The other researchers used a few additional methods, including vector normalization and second derivative.

The study measuring the color *in situ* during roasting [53] is especially interesting because of its relevance to the current project. To acquire the *in situ* NIR spectra, the researchers placed a fiber optic NIR probe 2 mm from the glass window in a home drum roaster and acquired a new spectrum every minute. The dataset used for PLS regression contained 52 samples, which is the smallest of the PLS datasets reviewed here. Color was measured *ex situ* with a colorimeter and correlated to the *in situ* NIR measurement from the time the sample was removed. The resulting PLS model had an R^2 of 0.94, which is comparable to the 0.925 achieved *ex situ* by Esteban-Díez et al. [25]. This was the second study published by Santos about *in situ* NIR, and the first did not perform as well [52]. The first study used *in situ* NIR to predict titratable acidity, analogous to the *ex situ* measurement of acidity performed by Esteban-Díez et al. [25]. The *in situ* model had an R^2 of 0.89 which as opposed to the 0.987 reported for the *ex situ* study. One explanation for this difference is that the first study by Santos used only mean centering as a pre-processing method, while the later study used SNV, first derivative, and second derivative. This suggests that the pre-processing method is very important to the predictive ability of the regression model.

1.3 Coffee Chemistry and Flavor

Coffee is often rated based on flavor categories. This is a useful way of handling the considerable complexity found in the chemistry of roasted coffee. The ability to measure flavor categories is of interest for two reasons. First, some flavors are directly linked to the degree of roast. The goal of choosing a roasting endpoint is to achieve the organoleptic characteristics associated with a desired roast level. Consequently, a scale for roast degree should be strongly correlated with the characteristics associated with each roast level. This provides a method for validating different roast degree scales. Second, the ability to alter flavors independent of roast degree by altering the roasting temperature-time profile gives the roaster greater control and provides an opportunity to improve the quality of the final product. Recent studies have suggested that NIR spectroscopy can be used to measure these properties in real time, making this level of control possible. Sweetness, acidity, body, aroma, bitterness are a few of the characteristics which are thought to be strongly affected by roasting and warrant further consideration for these purposes.

The main source of sweetness in coffee is sucrose, which has an initial concentration between 6% and 8% in green arabica coffee and has been shown to decrease throughout the roasting process [8]. Sucrose has successfully been measured on-line during roasting with NIR spectroscopy with a correlation coefficient of 0.93 [53]. While sweetness in coffee is an important attribute, it is often subtle, and many coffees display almost no perceived sweetness. Because of this, sweetness may not be a suitable attribute for validating roast degree, but the measurement of sweetness would be very beneficial in a complete *in situ* NIR coffee roasting solution.

Acidity is another important aspect of the flavor of coffee. Moderate levels of acidity create a pleasant effect also described as brightness or liveliness in the beverage, while high levels are described as sour, and coffee with low acidity is described as flat. Previous research has shown that the perception of sour is related to acids, and that titratable acidity is more correlated to sourness than pH [21]. Research specific to coffee compared the results of measuring titratable acidity at different pH endpoints and found that lower titration endpoints showed better correlation to perceived acidity, with correlation coefficients (R^2) increasing from 0.85 to 0.87 to 0.92 as the endpoint pH decreased from 8 to 7 to 6 [6].

The acid content of green coffee is mainly comprised of citric, malic, chlorogenic, and quinic acids [57]. During roasting, some acids break down and new acids are formed, including formic, acetic, glycolic, and lactic acids. Overall, this causes the

titratable acidity to increase early in the roast, then reach a peak and begin to decrease [6, 52]. This peak occurs early in the roasting process, before or near the typical endpoint of a light roast, so the perceived acidity is typically described as highest in light roasts and decreasing as the roast degree is increased [48].

The importance of acidity to perceived quality and strong correlation to roast degree make it a good potential indicator of roast degree and of interest as a quality parameter to monitor during roasting. A study has already applied *in situ* NIR to measure titratable acidity with an R^2 of 0.89, and two studies have successfully correlated perceived acidity from tasting panels to *ex situ* NIR spectra [26, 49, 52].

Body, or “the tactile feeling of the liquid in the mouth, especially as perceived between the tongue and roof of the mouth,” [47] may be the only attribute used to rate coffee which is not related to taste or smell. It is often used interchangeably with the term viscosity, although it is most likely not the same. In coffee, body is related to lipids, proteins, and polysaccharides and increases with roast degree, becoming highest in oily dark roasts before decreasing as the coffee becomes over-roasted [22, 49, 57]. This makes it a good candidate to use as a roast degree validation and *in situ* monitoring, provided it can be measured objectively. Measurements of body in coffee typically come from sensory evaluation, as the physical origin of this attribute is uncertain. Two studies have correlated sensory evaluations of body based on brewed coffee and espresso to NIR with R^2 values of 0.77 and 0.81, respectively [26, 49].

Bitterness is a very strong flavor in some coffees, with a primarily negative impact on quality. It can be caused by many different chemicals, but some of the main contributors in coffee are chlorogenic acids and their by-products [57]. Chlorogenic acid content is reduced as degree of roast increases, but some of the by-products remain and may even cause an increase in perceived bitterness. Robusta coffees have higher chlorogenic acid content than arabica coffees, and this has been proposed as the cause of their increased bitterness. Caffeine is also often associated with bitterness but may not be a major source. A study published in 1975 [32] compared the taste thresholds for individuals with high and low sensitivity to caffeine and found that the low sensitivity group cannot taste the levels present in brewed coffee, while the high sensitivity group can. Even with high sensitivity individuals, the study suggested that the contribution to bitterness may be small relative to other factors. Bitterness levels are generally considered to increase in dark roasts [22, 48], but due to variations in bitterness due to variety or processing, this may not be a good basis for validating roast degree. Bitterness was also correlated to NIR based on tasting panel results, with R^2 values of 0.76 and 0.86 [26, 49].

Aroma is the most complex aspect of coffee and is very important to its perceived quality [57]. Over a thousand volatile compounds have been discovered in coffee; most of these are formed in reactions occurring during the roasting process. Researchers have attempted to determine which of these components are aromatically active using gas chromatography-olfactometry (GCO) techniques, which involves a person smelling the effluent of a gas chromatograph [12, 51, 57]. This is necessary because the human nose is extremely sensitive to some compounds, detecting concentrations as low as parts per trillion. Most of the GCO studies consist of diluting the effluent until it can no longer be detected to determine a detection threshold and reporting the ratio of measured concentration to the detection threshold. Such studies have found fewer than 30 aroma-active compounds, but the specific set of aroma active compounds varies based on coffee origin, post-harvest processing, and roasting. The isolation techniques for determining aroma active compounds in coffee do not account for possible synergistic effects between compounds which could result in even more aroma-active compounds in the mixture that are not detected after isolation. Another issue which must be considered is the solubility of these compounds in water, which has been shown to result in an increased presence of polar aromatic compounds in brewed coffee relative to non-polar compounds [12].

Because of the extremely low concentrations at which aromatic compounds are often present, NIR spectroscopy is not an ideal method for detection. One technique which has been demonstrated for *in situ* detection of aromatic compounds during roasting is mass spectrometry (MS). *In situ* MS has been applied for process control and measurement of roast degree [20, 23, 29, 40, 60] and to measure individual components that contribute to aroma [5, 24, 33, 34]. The changes in aromatic compounds during roasting are complex and measuring changes in individual compounds is not sufficient for controlling roast degree and aroma. These studies often resort to chemometric techniques similar to those used in NIR to produce useful results from MS data.

1.3.1 Controlling Coffee Flavors with the Roasting Temperature Profile

The ability to control flavors and aromas independent of roast degree is of particular interest to roasters, and several studies have focused on this. These studies typically compare the effects of high temperature short time (HTST) roast profiles to low temperature long time (LTLT) profiles and keep the roast degree constant using either the

cracks, visible lightness, or Agtron number. The actual temperatures cannot be directly compared between studies because of differences in heat transfer effectiveness between roasters.

Aroma is the most common subject for comparison, which has a higher total intensity in the HTST roasts [30, 55]. When comparing the intensities by chemical class, pyridines, which are associated with unpleasant fishy aromas, increased in LTLT roasts, while ketones increased in HTST roasts, and total furans did not show significant change [44]. Comparing the aromatic composition of more varied temperature profiles (e.g. starting at high temperature and switching to low) revealed that the full temperature time history affects the volatile profile, and constant temperature profiles may not be sufficient [30]. Another study compared the composition of coffee roasted in a drum roaster and an air roaster with the same temperature profile and found that they generated the same volatile profile, which indicates that conclusions made based on one type of roaster can be applied to the other [5].

Studies comparing the effect of different temperature profiles on titratable acidity found that the acidity is highest in HTST profiles [30, 58]. The peak acidity, which occurs before the coffee reaches a light roast, decreases in HTST roasts, but the roasts used in making this conclusion were very fast, reaching the end of first crack in under 4 minutes [58].

Chlorogenic acids are of particular interest in coffee because they make up a high fraction of the green bean mass, around 6.5% for arabica and 10% for robusta [37]. They also have antioxidant properties and are associated with bitterness in brewed coffee [57]. Chlorogenic acids are highest in green coffee, and decrease with roast degree, reaching less than half their initial concentration in a light roast [30, 58]. Similar to titratable acidity, chlorogenic acids are highest in HTST roasts.

Sensory evaluations revealed that HTST roasts result in more oil migration and less burnt flavor, both of which make them more suitable for dark roasts [58]. All these results are interesting, but the lack of a consistent method of comparing roast degrees makes them less useful, as it is impossible to compare results between studies. The temperatures and times defining HTST and LTLT profiles also vary between different studies, so there are still considerable gaps which must be filled for a complete understanding of how coffee flavor can be controlled with the roasting temperature profile.

1.4 Objectives

The goal of this project was to improve the ability to control the roasting process and consistently achieve desired flavor profiles in the roasted coffee using online NIR. The primary focus was on roast degree, but the ability to measure flavor aspects in real time and control these independent of roast degree by changing the temperature-time roasting profile was also of interest. The following three objectives aided in obtaining this goal.

1. **Create a new roast degree scale based on the cracks.** The first objective is to use recorded audio during roasting to monitor the first and second crack events, capture the start and end times of these events, and predict these times with online NIR. These predictions will then be used to create a numerical scale for roast degree. First and second crack are already commonly used as references for roast degree in both commercial and home roasting, but the difficulty of predicting the start and end times of these events before they occur or even judging the times after they occur currently limits the usefulness of this technique. Using recorded audio to determine the exact times could be a useful and cost-effective tool for home roasters, and using NIR to predict the events will provide a robust measurement of roast degree for industrial roasters.
2. **Compare roast degree scales.** This consists of first developing a method for comparing roast degree scales based on one or more roast dependent sensory aspects of brewed coffee. Then, the objective is to create a simple roast degree scale based on NIR absorbance and compare this to the scale based on the cracks and to the industry standard roast degree based on visible lightness measured on the CIELAB color scale. This will test the hypothesis that visible lightness is not sufficient for measuring roast degree and NIR is capable of producing a more reliable measurement. Acidity and body are two aspects strongly associated with roast degree which have shown potential for being measured with NIR. Titratable acidity can easily be measured in a chemical lab, but body has only been measured by trained tasting panels. Lack of resources to perform tasting trials on the required scale will require exploring the possibility of measuring body based on physical or chemical measurements if it is to be used.
3. **Control coffee flavor independent of roast degree.** The final objective is to explore the ability to control flavor aspects of coffee at a given roast degree by changing the roasting temperature-time profile. Studies have found that different

roasting temperature-time profiles can affect the flavor and aroma. With the ability to measure roast degree *in situ*, it is possible to show the extent to which flavor aspects can be adjusted. This objective will focus on acidity as the flavor aspect to control and roast degree based on NIR darkness.

CHAPTER 2 Monitoring Coffee Roasting Cracks and Predicting with *in Situ* NIR Spectroscopy

2.1 Abstract

The prediction of start and end times of the first and second crack events in roasting coffee is feasible with *in situ* NIR spectroscopy. Roasting samples analyzed herein consist of eight varieties of arabica coffee with different origins and processing methods, roasted with four temperature-time profiles. Real-time analysis of recorded audio from coffee bean popping sounds provides a basis for determining the start and end times of each major event. A custom *in situ* diffuse reflectance probe improved NIR output, and PLS regression generated a separate model for each crack event. The resulting PLS models show strong potential for process control implementation. A newly developed roast degree scale based on the progression through crack events is arguably more meaningful than common color cues to connect and correlate the complex chemistries and consumer qualities in roasted coffee.

2.2 Introduction

Coffee roasting is a complex process involving three modes of heat transfer, elevated pressure, transient evaporation, and changes in material density and phase occurring at the same time as chemical reactions that produce hundreds of different chemical species [28, 57]. These processes occur on a wide range of time scales, depending on roasting conditions, with some roasts completing in under 10 min and others as long as 20 min or more. Even with the same heat application and quantity of coffee beans, differences in moisture levels, size, and chemical composition of the beans can cause the coffee to roast to a different level [13, 14]. This makes the ability to judge the roast degree in real time beneficial, but methods commonly used by roasters for this judgement, such as color, aroma, and sounds emitted (cracking or popping) during a roast, can be subjective and imprecise. One such method is based on the timing of the first and second crack events.

Two sets of popping sounds occur during roasting, referred to as first crack and second crack. First crack is often described as sounding like popcorn popping, and second crack is higher pitched and more frequent and numerous. These are used as a reference for degree of roast (light roast begins near the end of first crack, dark roast after the start of second crack). Beans are often observed to become oily soon after the start of second crack (Figure 1.1), and oiliness is an important distinguisher for dark roasts [48].

The causes of the cracks remain uncertain. First crack is often assumed to be caused by pressure from water vapor and carbon dioxide within the beans, and second crack is associated with oils migrating to the bean surface and sometimes attributed to fracturing of the cell matrix [48, 61]. Two articles studied coffee *in situ* with mass spectrometry and found spikes in caffeine and phenols during cracking but did not distinguish between first and second crack [23, 33]. Two more studies have used recorded audio during roasting to analyze the cracks, with the first study concluding that first crack is higher amplitude and lower frequency, while the pops in second crack occur at a higher rate [61]. The second study used neural networks to differentiate between the first and second crack, claiming a 100% success rate [62].

A difficulty that arises from using the cracks as a measurement of roast degree in small batches is the stochastic nature of the pops. The pops are caused by individual beans, and differences in the beans or temperature variations within the roaster can cause random variation in the times of the pops. Instead of attempting to listen for the start and end of these events, this variability could be reduced by recording audio during roasting and determining the time of each pop. Then with the full set of pop times, the start and end of the events can be determined in a way that is not affected as drastically by any single pop.

Even with the consistency gained with recorded audio, it is impossible to know when the cracks will happen before they start, which is problematic when attempting to use the cracks to judge the endpoint of roasts which fall between the first and second crack, as do most light and medium roasts. This study will attempt to reduce this uncertainty by predicting the start and end times of the events with *in situ* near infrared (NIR) spectroscopy.

Multiple studies have used NIR to predict roast degree metrics, including color, density, weight loss, and moisture content [2, 9, 25, 53]. Only one study [53], measured color *in situ* with a correlation coefficient of 0.89. Several recent studies have measured other aspects of coffee with *in situ* NIR, including acidity, sucrose, roasting disturbances, and antioxidant properties [15, 16, 52, 53]. Roast degree has also been

measured based on color with NIR hyperspectral imaging [18].

The objectives of this research were to use audio recordings to determine the start and end times of the first and second crack events during roasting, to use *in situ* NIR spectroscopy with partial least squares (PLS) regression to predict the start and end of the cracks, and to develop a numerical scale for roast degree (viz., a quantifier for the more generic but typical light-medium-dark reference terms) based on the PLS results. Samples consisted of eight coffees of different origins roasted with four different temperature profiles, and a new metric derived from the spectra, called NIR darkness, aided in analysis.

2.3 Methods

2.3.1 Coffee Roasting

A Fresh Roast™ SR500 air roaster (Home Roasting Supplies, UT, USA) modified for temperature control up to 250 °C and fan power control (0-24 VDC) roasted the coffee, and an application developed in MATLAB controlled the roaster and collected data, including time, inlet temperature, outlet temperature, heater power, and fan power. Thermocouples measured air temperature entering and exiting the roasting chamber, and adjustments in heater power controlled the inlet air temperature.

Table 2.1: List of coffee varieties used in this study

	Coffee Origin	Processing Method
1	Honduras	Washed
2	Ethiopia	Washed
3	Brazil	Natural
4	Kenya	Washed
5	Indonesia	Washed
6	Guatemala	Washed
7	Colombia	Washed
8	Ethiopia	Natural

Roasting samples consisted of eight arabica coffee varieties (Table 2.1) selected from different regions and included washed and natural processing methods. The focus of this study was on improving the ability to produce high quality specialty coffees,

which typically only consist of the arabica variety. Roasts consisted of only one variety, under the assumption that blending could be performed after roasting. Each roast contained 120 g of green coffee.

Each variety ran with four different temperature-time profiles, which were designed to mimic industrial roasts (Figure 2.1). In profiles 1 and 2, the roast ended after the end of second crack, in profile 3, it ended after the start of second crack, and profile 4 ended approximately midway between the first and second cracks. Profiles 1 and 2 start at the same temperature and then deviate at 300 s, with profile 1 increasing slowly and staying below 220 °C, and profile 2 quickly exceeds 220 °C to capture the difference between fast and slow dark roasts. The cracks become less pronounced in low temperature roasts (below 200 °C), which limits the extent to which the roast could be slowed down. Profiles 3 and 4 were designed to capture the difference between profiles which increase more slowly in the early stages of the roast.

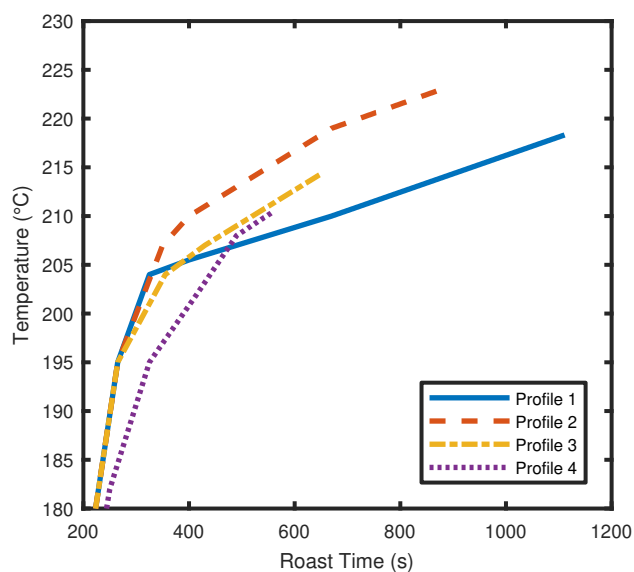


Figure 2.1: Inlet air temperature-time profiles used in roasting

2.3.2 Crack Detection

A microphone (CVL-1064, Cyber Acoustics, WA, USA) placed 5 cm from the air outlet of the roaster recorded audio, and a MATLAB application analyzed the audio. The application split the audio into 0.01-second intervals and performed a Fourier transform on the data then averaged the amplitude of all frequencies between 4 and 7 kHz. The algorithm counted a pop for any value more than twice the previous value. The average times of the first and last five pops in each cracking event marked the start

and end of the event, respectively.

2.3.3 *In Situ* NIR

A Si-Ware NeoSpectra SWS62221-2.5 Fourier transform NIR spectrometer (Si-Ware Systems, Egypt) with a range of 1350-2500 nm captured *in situ* diffuse reflectance NIR spectra through a 550 μm diameter, 0.5 m long low OH fiber optic cable (Thorlabs, Inc.) placed at a 3 cm distance from the side of the roasting chamber (Figure 2.2). Before each roast, the spectrometer recorded three background spectra against a solid PTFE cylinder placed inside the 1.5 mm thick glass roasting chamber. Two 50 W halogen bulbs placed at a 45° angle from the fiber probe illuminated the chamber, and the spectrometer captured a new NIR spectrum every 10 s during roasting. This differs from the setup used in previous *in situ* NIR studies, which have placed the probe at a distance of 2 mm from the roasting window [15, 16, 52, 53]. The increased distance allows a larger area of the sample ($\approx 6 \text{ cm}^2$) to be captured by the probe, resulting in improved averaging of inconsistencies in the coffee, but also requiring a more intense light source.

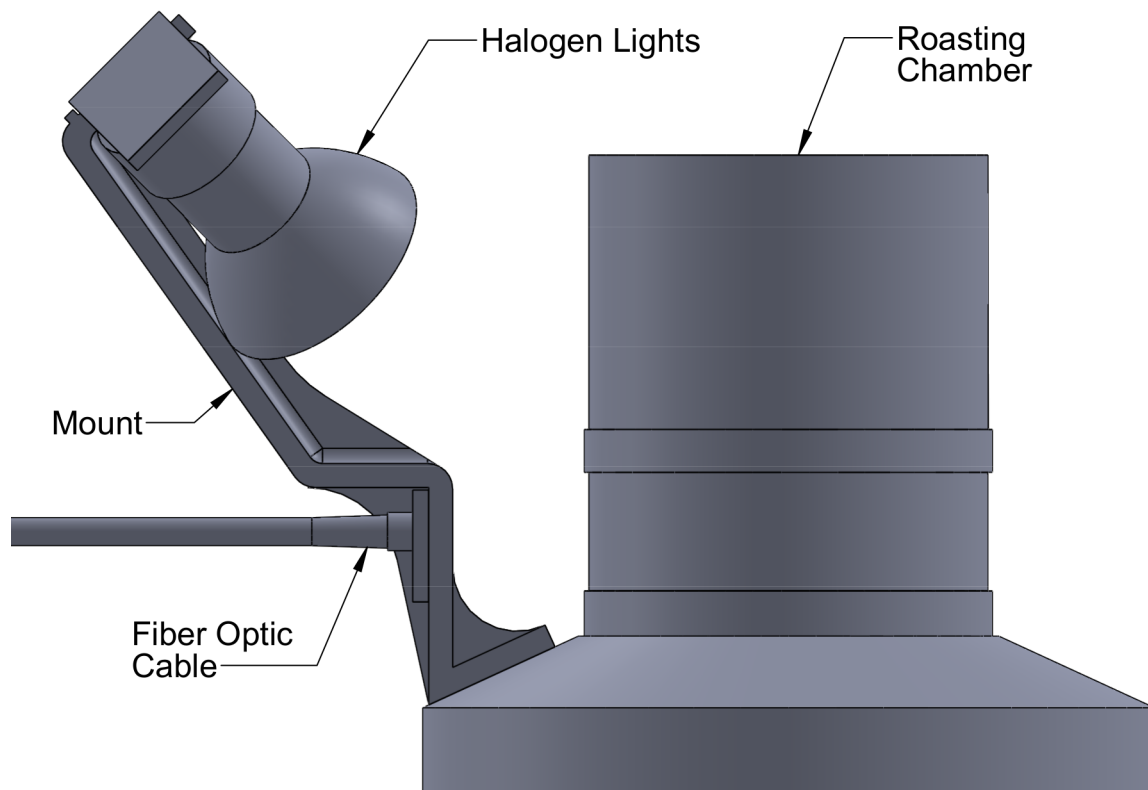


Figure 2.2: Schematic of the roaster with NIR mount

2.3.4 NIR Data Analysis

The NIR spectra underwent first-order Savitzky-Golay filtering in time with a window of 14 points preceding the current time for noise reduction [54]. This effectively applied a linear regression to the last 140 s of data for each wavelength to provide a value for the current time. The window size selection was based on the performance of the final PLS models as there was a trade-off between noise reduction and responsiveness. Although Savitzky-Golay is more commonly used in filtering across wavelengths, the continuous acquisition of spectra used in this study also opened the possibility to filter each wavelength in the time direction.

PLS regression in MATLAB utilized the libPLS library with autoscaling as the selected pretreatment method and the leave-one-out method for cross-validation [39]. Additional pretreatment methods of interest included multiplicative scatter correction (MSC) and orthogonal signal correction (OSC), but these were not used in the final models. Analysis resulted in four separate PLS models, with one for each event (first crack start, first crack end, second crack start, and second crack end).

The response variable (Y) for PLS regression is a continuous value which needs to depict the proximity to the crack event of interest at the time an NIR spectrum originated. If time were used for this variable, the result from the PLS model would be the number of seconds before or after the crack event. The problem with this approach is that the number of seconds is dependent on the temperature profile and cannot be accurately judged from the NIR data alone. Instead, the response variable was generated from NIR absorbance values (see section 2.4.2).

To optimize the accuracy of each model near the event of interest, the datasets included only spectra close to the event. To achieve this, the cutoff for each model was the previous and next event (e.g. the first crack end data set ranged from the start of first crack to the start of second crack). If another crack event was not available as a limit, a fixed limit of 100 s from the event became the cutoff, but the cutoff never exceeded the start of the cooling sequence. Although spectra from every 10 s were available throughout each roast, the filtering in time caused adjacent spectra to be co-dependent, which is not conducive to good regression models. To mitigate this the dataset included only one in every three available spectra, resulting in a 30-second separation between spectra.

Randomly spitting the full dataset into 80% and 20% generated calibration and prediction datasets, respectively. A separate prediction data set is used after the creation of the PLS model to test the results and check for overfitting by comparing the

root mean square error of calibration (RMSEC) to the root mean square error of prediction (RMSEP). The coefficient of determination (R^2) and range error ratio (2.1) are additional test statistics generated from the prediction dataset for this study.

$$RER = (y_{max} - y_{min})/RMSEP \quad (2.1)$$

2.4 Results and Discussion

2.4.1 Sound Analysis

The ability to determine automatically whether the current event is part of the first or second crack was of interest but did not prove to be possible with the methods applied here. When listening to the cracks, there is a discernable difference in the frequency of the sounds, with second crack having a higher frequency than first. The Fourier transforms (Figure 2.3) of the sounds did not consistently show a difference in the frequency of the two types of pops, so programmatically determining the type of pop was not feasible. The peak frequencies observed in this research for both first and second cracks were between 4 and 7 kHz. This differs significantly from previous research, which reported the peak frequency from first crack at 800 Hz and second crack at 15 kHz [61]. While the current research confirmed a higher amplitude for first crack and a higher rate for second crack, both quantities displayed too much variation to be useful in separating the two events. Instead, the method chosen for discriminating between them was to manually input a time range for each event and then allow the MATLAB app to determine more precise start and end times.

The crack detection algorithm results in a list of times for the individual pops in the first and second crack, which can be used to determine the start and end times of the events. Because of the stochastic nature of the pops, using the first and last pop as the start and end of the event would result in too much variance in the event times. A set of crack data from 12 roasts for first crack and 5 roasts for second crack allowed several methods for using the complete set of pop times to determine the event start and end times to be explored. Methods included first and last pop, a formula based on the average and standard deviation of all the pop times, and using the average of the first and last five crack times as the event start and end times. The latter method showed the most success in representing the events while reducing the dependence of the start and end times on individual cracks. Both events tail off at the end (Figure 2.4), which can cause increased variability in the end time of the events

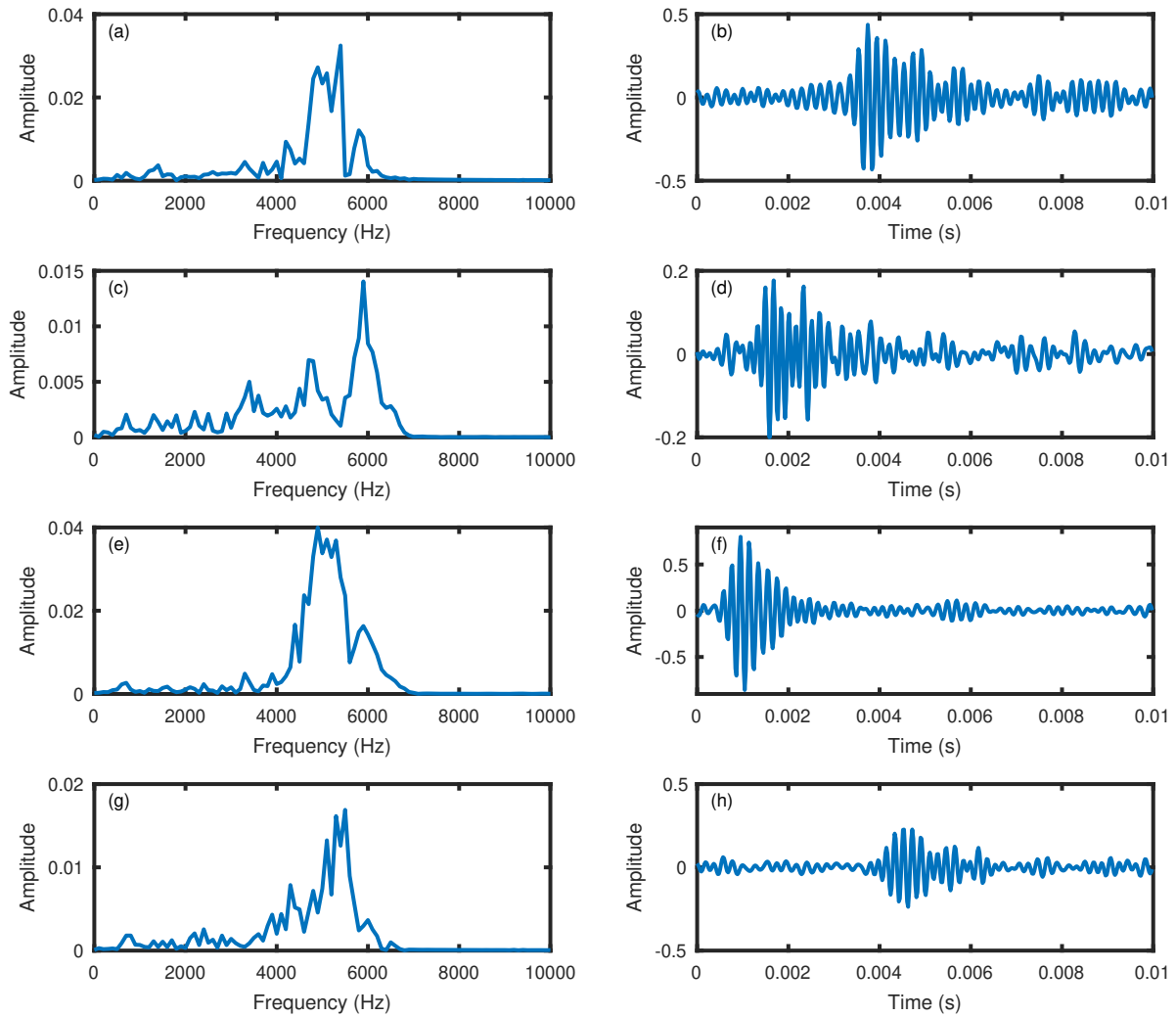


Figure 2.3: Fourier transform (left) and raw audio data from two first crack sounds (a-d) and two second crack sounds (e-h)

based on the timing of the last few random cracks. The number of pops detected in the 120 g (approximately 700 coffee beans) test batches roasted in these experiments had an average of 48 pops in first crack and 93 in the second. The small number of cracks observed caused some variation in the measurement of the start and end times measured, especially at the end of both events where a tail is observed in the distribution. The number of pops observed increased with roasting temperature for both first and second crack.

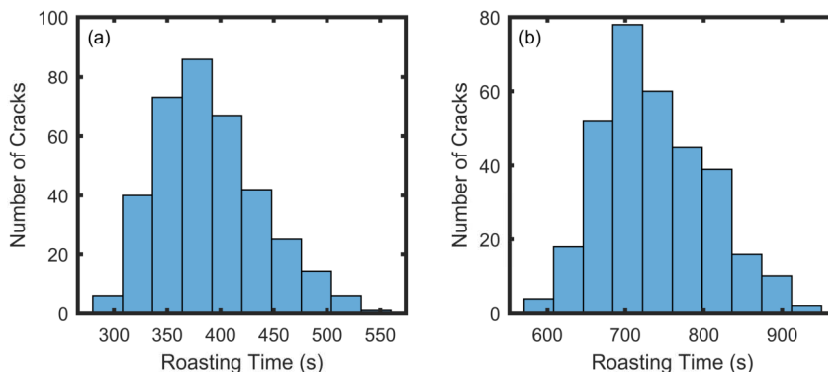


Figure 2.4: Histograms of first crack times from 12 roasts (a) and second crack times (b) from 5 roasts

2.4.2 NIR Spectra

As mentioned in section 2.3.4, a PLS response variable needed to be generated from NIR absorbance to provide a continuous measure of proximity to each event. The criteria identified for this variable were that it should change continuously throughout the roast and have a minimal amount of random variation. To avoid random variation, averaging a section of wavelengths proved to be helpful. Most of the NIR wavelengths (Figure 2.5a) decrease in absorbance during roasting, but the change in absorbance levels off in dark roasts, which is not ideal. The far-left region of the spectrum (1300-1400 nm or $7692\text{-}7142\text{ cm}^{-1}$) can be seen to increase in absorbance toward the end of the roast, so subtracting this from a region on the right side helped to counteract the leveling off. Based on these observations, the response variable was generated by subtracting the mean absorbance between 7692 and 7142 cm^{-1} from the mean absorbance between 6667 and 6250 cm^{-1} . The resulting value was termed NIR darkness (Figure 2.5b), which decreases with roast degree, contrary to darkness in the visible spectrum. This NIR darkness is essentially a measure of roast degree, with arbitrary units, and performed better in the PLS models than a single NIR wavelength. The remaining step in generating the response variable was to subtract the NIR darkness at the crack event of interest (e.g. the start of first crack) from the current NIR darkness, resulting in the NIR darkness offset value, which is positive before the event, zero at the event, and negative after the event.

Spectral pre-processing with MSC is helpful in visualizing local changes in the dataset (Figure 2.6). Seven regions with different features are labeled, and the most active regions based on the change in absorbance are I ($7700\text{-}7100\text{ cm}^{-1}$), II ($7100\text{-}6600\text{ cm}^{-1}$), V ($5500\text{-}5000\text{ cm}^{-1}$), and VII ($4650\text{-}4000\text{ cm}^{-1}$). Regions II and V are

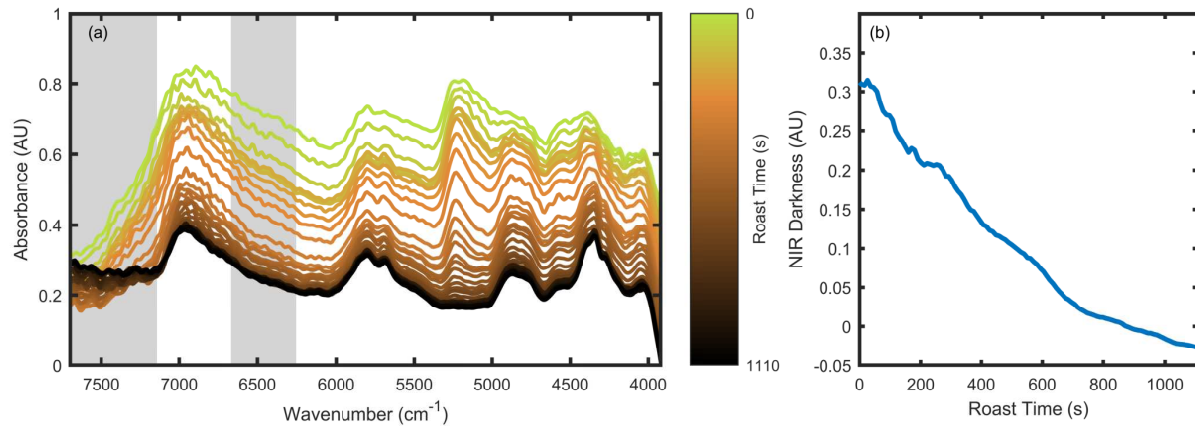


Figure 2.5: Time-series-spectral-overlay after Savitzky-Golay filtering taken during a roast with the wavelengths used in the NIR darkness predictor ($7700\text{-}7142\text{ cm}^{-1}$ and $6667\text{-}6225\text{ cm}^{-1}$) highlighted. (a). The resulting NIR darkness value vs time throughout the roast (b).

associated with water which decreases during roasting [2, 26]. Other regions have been associated with the major components of coffee based on the vibrational frequency of chemical bonds or by separating the components and measuring their NIR spectra, but there is a significant amount of overlap between the components, making it difficult to attribute NIR peaks to specific components [49].

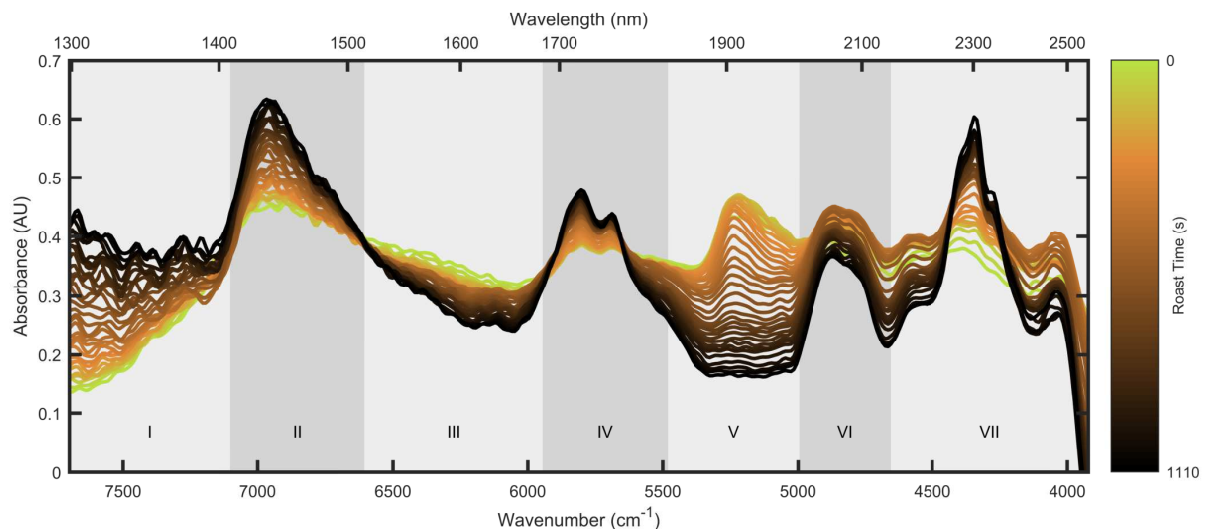


Figure 2.6: MSC treated time-series-spectral-overlay with regions-of-interest labeled

The coffee NIR spectra observed in this study differ slightly from previous studies, especially in region VII [2, 52], attributed to unique probe geometries, to the method for background reference methods, and to the result of high temperatures used in

roasting. In this study, the reference was taken using a block of PTFE inside the glass roasting chamber.

To explore the effect of temperature on the NIR spectrum of coffee, it is useful to look at spectra taken at the end of the roast during cooling. The cooling phase consisted of turning off the heat and leaving the fan running to force room temperature air through the coffee. Figure 2.7 shows the change in absorbance after 60 seconds of cooling, during which time the coffee cools from 220 °C to below 100 °C. The rate of cooling is fast enough that the effects of continued roasting reactions should not be a major factor, and a significant change in absorbance is seen from 5000 cm^{-1} to 4000 cm^{-1} . Reducing the intensity of the light source by replacing the two 50 W bulbs with a single 20 W bulb increased this effect while the high wavenumber range was unaffected. This leads to the conclusion that the change is likely due to increased emission at elevated temperatures as opposed to temperature dependence of reflectance. The features found at 7000 cm^{-1} and 4900 cm^{-1} are more likely due to a change in reflectivity, because they become more prominent with the more intense light source.

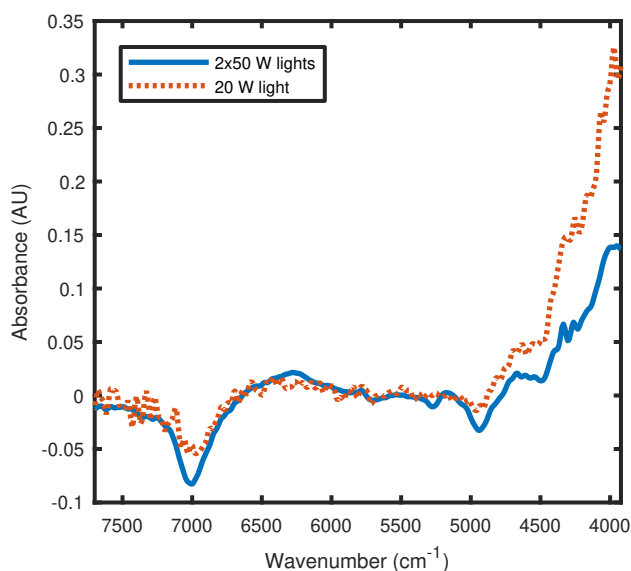


Figure 2.7: NIR spectrum before cooling subtracted from the spectrum after 60 s of cooling comparing two light source intensities

2.4.3 PLS Models for Crack Prediction

Selection of pretreatment methods was based on their impact on the RMSE and R^2 values of the PLS models. The first pretreatment applied was Savitzky-Golay filtering in time, with a window size of 14 spectra. The window only included past spectra

Table 2.2: PLS regression results. The number of points for each model is different because of the selection criteria and includes both calibration and test data. ⁽¹⁾Range Error Ratio

Event	Points	Y Min	Y Max	PLS Components	RMSEC (AU)	RMSEP (AU)	R ² Prediction	RER ⁽¹⁾
First Crack Start	213	-0.0788	0.0730	6	0.0061	0.0068	0.95	22.2
First Crack End	238	-0.0895	0.0772	8	0.0080	0.0091	0.92	18.3
Second Crack Start	191	-0.0875	0.0818	4	0.0042	0.0041	0.99	40.9
Second Crack End	134	-0.0094	0.0892	5	0.0060	0.0070	0.93	12.7

to insure this filtering would be possible in real time. Time filtering combined with a 10 s acquisition interval provided two benefits over the use of a longer window which would not require filtering. First, it allows more frequent updates, which is beneficial when using NIR to control the roasting process, and second, it allows more flexibility in choosing the filtering time window that provides the best performance without affecting the data acquisition window. Although some noise was visible in the wavelength direction after applying the time filter, applying Savitzky-Golay filtering across wavelengths did not improve the PLS results. The final models used MSC pretreatment, but not OSC, which failed to provide improvement in the results. The analysis also explored using roast time as the response variable (Y) for generating the models instead of NIR darkness. This would result in the models predicting the number of seconds from the start and end of the cracks instead of the less useful NIR darkness number, but the performance of the models suffered with this method. This is partially because the time to the start and end of each crack event is dependent on the temperature-time profile, which is not information contained in the NIR spectrum.

The results of the four models (Table 2.2 and Figure 2.8) varied in quality, but all met standard minimum acceptance criteria [1]. An RER above 10 is recommended for quality control and above 15 for quantification. All four models met the quality control minimum, and only the second crack end model failed to meet the minimum for quantification. The number of PLS components selected ensured that there was not a large discrepancy between the RMSEP and RMSEC and the ratio did not exceed the recommended maximum of 1.2.

The two crack start models performed better than the crack end models, which is likely because the pops tail off at the end of both events, resulting in greater variance in the observed end times. The model for start of second crack displayed the best fit,

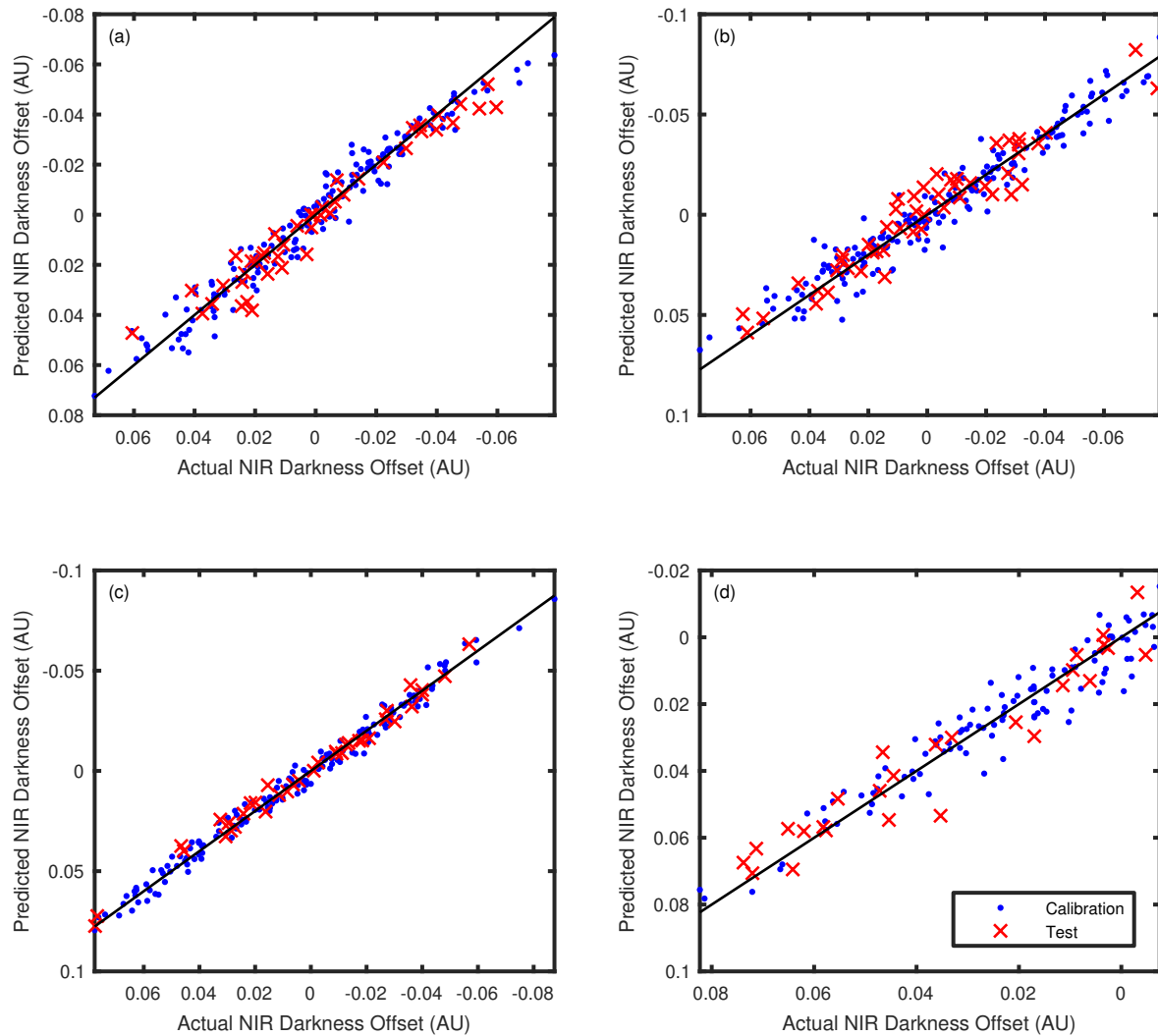


Figure 2.8: Prediction plots of PLS models vs measured NIR darkness offset (AU) values. Values represent the change in NIR absorbance which will occur before the event of interest. A value of 0 occurs at the event, positive values before, and negative after. The four plots represent first crack start (a), first crack end (b), second crack start (c), and second crack end (d).

with an R^2 of 0.99. This may be because of the appearance of oils on the bean surface at the start of second crack, which would be expected to cause a distinct change in the NIR absorbance at this time. In contrast, if first crack is caused by the sudden expansion of water vapor in the center of the bean, this may not have as much impact on the NIR spectrum observed at the surface. For the purposes of monitoring and controlling the roast and determining the desired endpoint, the ability to predict the end of first crack and the start of second are more important than the others, because most roasts end between or near these events. Light roasts typically complete near

Table 2.3: Reference numbers used in defining a roast degree scale based on the crack events. A roast ending between two events receives a roast degree between the two reference numbers. The exact value is determined by the output of the PLS models.

Event	Roast Degree
First Crack Start	-100
First Crack End	0
Second Crack Start	100
Second Crack End	200

the end of first crack, medium roasts between the two cracks, and dark roasts during the first half of second crack, but rarely to the end [48].

2.4.4 Numeric Roast Degree Scale

Developing a numeric roast degree scale made the results of the PLS models more useful in real time, allowing the results to be displayed as a single number instead of four. Arbitrary numbers were assigned to the start and end of cracks as a reference for this scale (Table 2.3). Herein, a roast ending at that start of first crack (much lighter than most roasters would ever go) will have a roast degree of -100 (arbitrary units), and a roast ending at the end of first crack would be 0 (a typical start point for many light roasts). Roasts falling between two events are assigned a roast degree by interpolation between the two reference numbers, using the PLS model output to determine the exact value. For example, a roast ending during second crack with a second crack start output of -0.02 and a second crack end output of 0.03 has a roast degree of 140, as shown in equation (2.2). A more detailed example can be found in Appendix J. On this scale, light roasts would typically fall between 0 and 50, medium from 50 to 100, and dark roasts above 100. The use of this scale requires that the proximity to the next event be known, which is only made possible in real time with the values produced by the PLS models.

$$RoastDegree = 100 + 100\left(\frac{0.02}{0.03 + 0.02}\right) = 140 \quad (2.2)$$

The result of this scale is shown in Figure 2.9, comparing the result of the PLS models to the values measured based on recorded audio and NIR darkness. The primary source of noise is variations in the coffee beans passing in front of the sensor, so

increasing the size of the viewing window would decrease the influence of these fluctuations and increase the prediction accuracy. This would be possible using a larger roaster than the one in these experiments but would also require a larger diameter fiber optic probe cable to supply enough light.

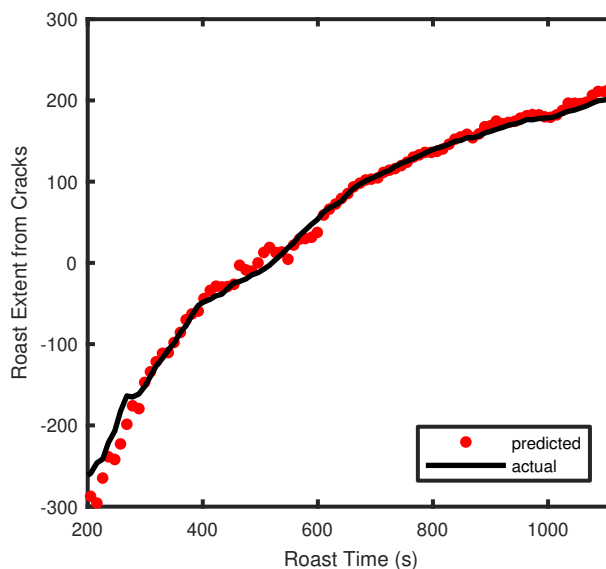


Figure 2.9: Roast degree predictions from *in situ* NIR compared to actual roast degree from crack times measured with a microphone

2.5 Conclusions

Based on PLS regression with audio recordings from coffee roasting, *in situ* NIR spectroscopy provides a reasonably accurate measuring technique for the prediction of the start and end times of first and second crack events, which are key system state indicators for a vast majority of desired roasting outcomes. The predictive model then becomes the basis for establishing a new roast degree scale that can provide better objectivity. This new roast degree provides a numerical scale to represent the progression through characteristic events in the roasting process for a more consistent comparison of coffees with different origins and from different roasters. Additional work is required to compare this scale to other common methods of measuring roast degree, such as color and Agtron number, to be thorough in demonstrating the full range of benefits and potential shortfalls of this new roast degree for industry and consumer needs.

CHAPTER 3 Online Determination of Coffee Roast Degree toward Controlling Acidity

3.1 Abstract

Three methods of measuring coffee roast degree are compared using titratable acidity as an indicator of roast-dependent flavor change. The first roast degree method was based on the cracks, the second was based on NIR absorbance, and the third was the common L^* value from the CIELAB color space in the visible spectrum. Roasting trials utilized arabica coffee from eight origins in an air roaster. A second dataset with constant temperature roasts showed how acidity can be controlled by changing both the roasting temperature and roast degree, finding the linear effects of roast time and roast degree on acidity.

3.2 Introduction

Roast degree is the primary descriptor of roasted coffee and often the first consideration consumers consider when buying coffee, though there is no consensus on how roast degree should be measured. The most common method is based on visible color or lightness, determined visually or with color analyzers measuring on the CIELAB color scale [36].

Unfortunately, the color of coffee is affected by factors other than roast degree, such as the green coffee processing method, with dry processed coffees requiring more time or higher temperatures to reach the same color as wet processed coffees [37]. Additionally, research has shown that the relationship between color and mass loss is different depending on the roasting temperature-time profile [29, 46]. These observations indicate that color is not the best attribute on which to judge roast degree.

Several methods in addition to color have been used to determine roast degree. The change in mass or density provides an indication of the cumulative chemical change, and the water loss is often subtracted from the weight loss to give a value called roast loss [37]. Because these methods cannot easily be applied on-line, they

are not useful for controlling the roast in real time, but they could be made useful by predicting with NIR spectroscopy [2]. Studies have also demonstrated the possibility of determining roast degree based on statistical analysis of volatile compounds evolved from the coffee [20, 23, 29, 40].

The first and second cracks, which are two sets of popping sounds typically occurring at different times during the roast, may be the most common method for determining roast degree in real time. By itself, this method is subjective and difficult to judge consistently, but the subjectivity can be removed by predicting the crack events with *in situ* NIR spectroscopy and using the result to generate a numeric roast degree scale (see Chapter 2).

Although there is evidence that visible color is deficient for measuring a robust extent of roasting that is objectively consistent for taste, demonstrating the suitability of another roast degree scale requires a more rigorous method of comparison. Since the aim of roast degree is to communicate the roast-dependent flavor and aroma changes in coffee, it would make sense to use measurements of a coffee flavor attribute to compare roast scales.

Some important flavor attributes used for rating coffees include body, aroma, and acidity [47]. Body is the tactile feeling of coffee in the mouth [47] and is generally thought to increase during roasting from light to dark roasts, although it decreases again in very dark roasts [22]. While it might make a good reference for comparing roast degree scales, it is typically determined by sensory panel evaluation, and an attribute that can be measured based on physical or chemical measurements is preferred [49]. Aroma also changes with roast degree, though due to a large variety of chemical compounds generated in small quantities at different times in the roast [57]. This would make comparing coffees of different roast degrees by aroma difficult. Acidity, which can be measured by titration, initially increases during a roast, then reaches a peak and begins to decline [6, 52]. Most roasts end at some time after this peak such that the acidity is typically considered to decrease monotonically with increasing roast degree. The strong association with roast degree and simplicity of measurement makes acidity an ideal attribute for comparing distinct roast degree scales.

Studies have shown that acidity is affected by roast temperature in addition to its dependence on roast degree [30, 52, 58]. This is done by comparing the acidity of high temperature-short duration roasts with low temperature-long duration roasts while keeping the roast degree constant based on either the crack events or color measurements. The results of these studies allude to the possibility of controlling acidity at a given roast degree by altering the roast temperature profile, but additional

data are required to quantify the extent to which acidity can be altered across different roast degrees and varieties of coffee. This is an area where the quality and quantitative accuracy of the roast degree scale are important, as it is used to differentiate the effect of roast duration from the effect of roast degree. Other studies that have compared coffee attributes under different roasting profiles at the same roast degree primarily focused on volatile compounds and aroma [5, 44, 55].

The objectives of this research were to use titratable acidity from roasted coffee to compare three roast degree scales and to use the best scale to explore the ability to control acidity with the roasting temperature-time profile. These three scales consisted of a simple scale based on NIR absorbance, a numerical scale generated from predictions of the start and end times of the first and second cracks with *in situ* NIR, and visible lightness from the CIELAB color space. A new method of scaling the acidity by the peak acidity for each coffee variety facilitated the comparison of titratable acidity results from multiple varieties of coffee.

3.3 Methods

3.3.1 Roasting and Sampling

The roaster modifications and coffee varieties are described in section 2.1.1. The same set of four roast profiles designed to simulate industrial drum roasts were used to generate the dataset for comparing roast degree scales, with four samples removed during each roast for acidity and color measurement. A separate set of constant inlet temperature roasts generated the acidity control data set, with two samples removed at selected roast degrees during each roast.

The fan power profile for each roast was slow enough that the lid could be removed for sampling at any point in the roast without losing a large number of beans. A small metal spoon removed 12-15 g of coffee for each sample, which was then placed in an identical roasting chamber and cooled with room temperature air. The dataset consisted of samples from eight varieties of coffee with four roasts per variety. After roasting, a burr grinder (Cuisinart CBM-18N) ground the samples at the smallest grind setting, at which 80% of the grounds could pass through a #40 sieve (425 μm).

3.3.2 *In Situ* NIR

The methods for measuring and analyzing *In Situ* NIR were the same as described in section 2.3.3.

3.3.3 Ground NIR

A custom 3D-printed ground coffee diffuse reflectance probe allowed a large surface area of ground coffee to be captured by the fiber optic cable for the spectrometer. The 12-mm deep, 64-mm diameter sample tray exposed a surface area of 32 cm² of coffee. Two 20-W halogen light bulbs with a color temperature of 2700 K illuminated the sample. A 0.5-m long 550- μ m diameter low OH fiber optic cable (Thorlabs Inc., NJ, USA) placed 90 mm above the sample surface carried light to the spectrometer. Three measured spectra were averaged for each sample.

3.3.4 Lightness Measurement

A portable color analyzer (CTI, China) with an 8-mm diameter viewing window measured lightness of the ground coffee samples in the CIELAB color scale (CIE, 2004). The reported lightness values are averages of five samples.

3.3.5 Titratable Acidity

The standard method detailed by the Association of Official Agricultural Chemists in AOAC 920.92 provided a basis for the titratable acidity procedure [4]. A 30-mL volume of 80% ethanol extracted acids from 4 g of coffee at room temperature for 16 hours, after which the samples were filtered and diluted to 150 mL with water. The titration was performed using a pH probe with a pH of 7.0 as the titration endpoint instead of phenolphthalein indicator. The samples were titrated with 0.05-M NaOH, and the result was reported as the volume of 0.1 M NaOH required to neutralize a 100-g sample of coffee (as specified in the AOAC method). A set of 6 repeat titrations resulted in a measurement standard deviation of 10 mL of 0.1 M NaOH/100 g.

3.4 Results and Discussion

3.4.1 NIR Roast Degree

In Chapter 2, a quantity called NIR darkness provided the basis for measuring the distance from the crack events. The selection of this property was based on its monotonically decreasing behavior throughout the roast. Figure 3.1 shows some wavelength ranges explored for deriving this quantity from the full set of spectra in Figure 2.5. Averaging the absorbance of ranges 100 nm wide reduced the noise from the spectrometer and simulated the measurement that could be obtained with single color

NIR LEDs in a simplified sensor design that might be produced at far lower cost than implementing a full NIR spectrometer. Three ranges were evaluated for their unique characteristics and suitability to such a designing such a sensor.

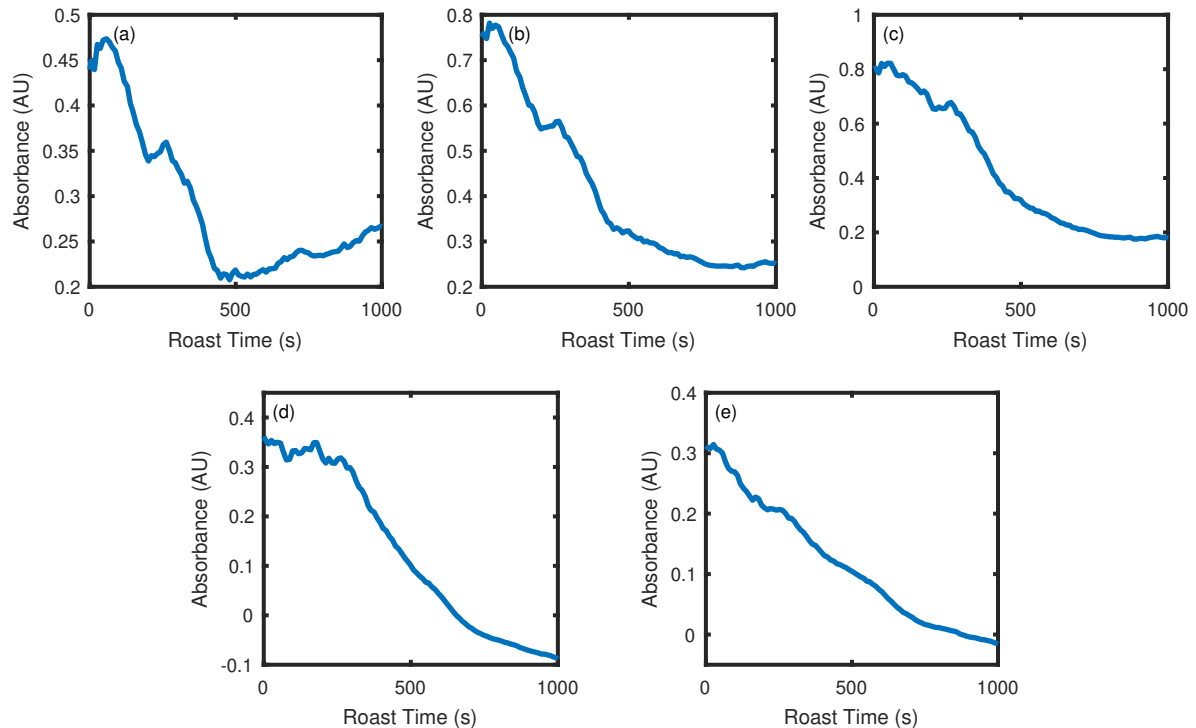


Figure 3.1: Mean NIR absorbance over three wavelength ranges: 1300-1400 nm (a), 1500-1600 nm (b), and 1900-2000 (c) and the absorbance resulting from subtracting two ranges: c-a (d) and b-a (e).

Although these spectra come from a single roast, the behavior was consistent when observing data from other coffee varieties or roast profiles in this study. The first range selected of 1300-1400 nm ($7692\text{-}7143\text{ cm}^{-1}$) decreases initially and then begins to increase near 500 s into the roast. This would make the range a poor choice for a roast degree scale, as it would produce the same value at two different times. An additional inflection can be seen near 200 s, which can be observed in all three of the wavelength ranges to some extent. The second and third ranges evaluated were 1500-1600 nm ($6667\text{-}6250\text{ cm}^{-1}$) and 1900-2000 nm ($5263\text{-}5000\text{ cm}^{-1}$), respectively, which primarily decrease throughout the roast but flatten out at the end. Again, this change in rate would not be an ideal behavior for a simple roast degree scale because of the difficulty in differentiating dark roasts in particular. Subtracting the 1300-1400 nm range from one of the higher ranges addresses these issues, keeping the value from flattening out at the end in both cases. The approach found the best result with

the middle wavelength range (3.1e), which removed the shoulder at 200 s and shows a more constant slope early in the roast (before 300 s), whereas the higher range (3.1d) appeared noisy early in the roast.

The resulting value is referred to as NIR darkness and is obtained by subtracting the average absorbance of 1300-1400 nm from 1500-1600 nm. This results in a roast degree scale capable of differentiating roasts at any level in real time rather than grinding samples offline.

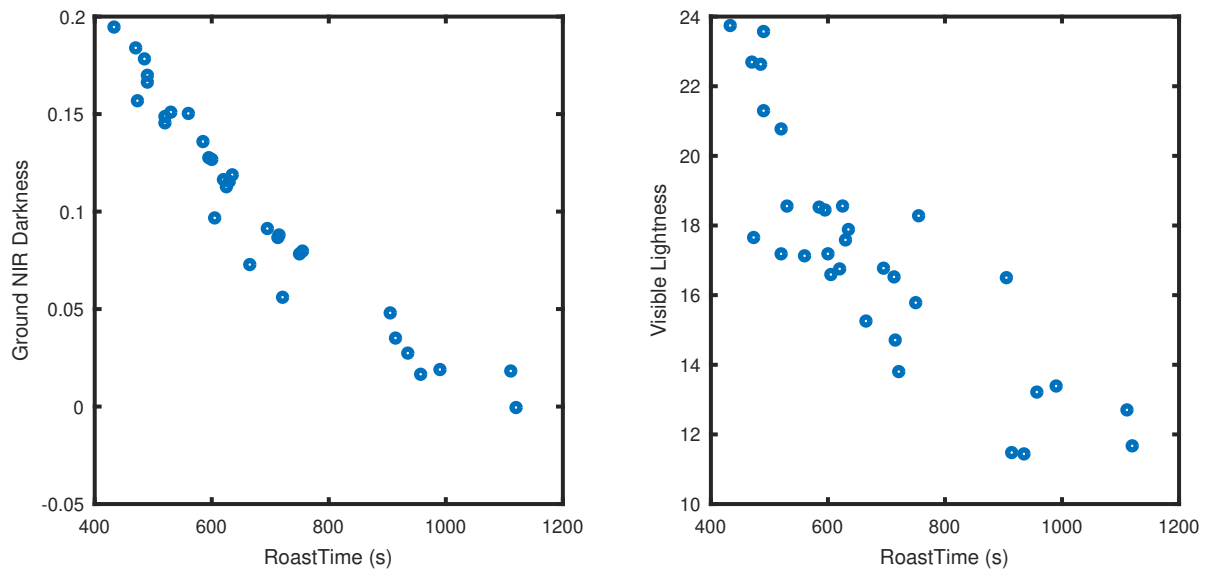


Figure 3.2: NIR darkness (a) and visible lightness (b) plotted against time for all eight coffee varieties roasted with profile 1.

3.4.2 Comparing NIR Darkness to Visible Lightness

Plotting NIR darkness and visible lightness values measured on ground coffee samples (Figure 3.2) against roast time for a single roast profile highlights the differences between the two scales. The most noticeable difference is that NIR darkness displays a lower level of noise. Although these plots include eight different varieties of coffee, which cannot be expected to roast at the same rate, the increased consistency seen in the NIR darkness plot provides evidence that improvement over that visible scale can be achieved. This indicates that NIR darkness is less affected by differences in coffee varieties, and instead is displaying the result of changes occurring during the roast.

3.4.3 Comparing Online and Ground NIR Darkness

NIR darkness values can be measured either *in situ* based on the whole beans in the roaster or after roasting and grinding. Ground coffee measurements are a more direct comparison to lightness measured on ground coffee (Figure 3.2), but online roast degree measurements are more useful when controlling the roast. The online and ground measurements (Figure 3.3) have a very strong correlation (coefficient of 0.99). Therefore, the remaining results will use online measurements to validate conclusions for roast degree measurement.

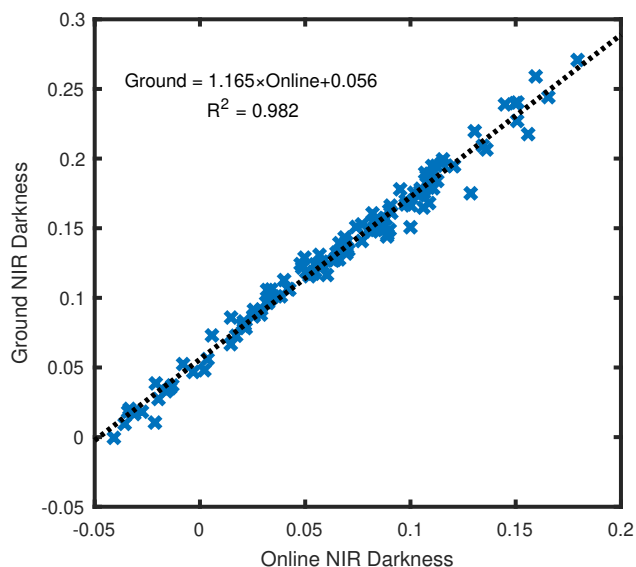


Figure 3.3: Comparison of NIR darkness values measured online vs offline ground.

Although the correlation between online and ground NIR is strong, the difference may still be useful to roasters. Agtron[®] roast analyzers, which are commonly used in industry and base their measures on NIR, allow the roast degree to be compared between whole bean and ground coffee. The difference is considered to measure the development of the roast. If the whole bean measurement results in a darker roast than ground samples, this indicates that the coffee may be underdeveloped, or roasted too fast so that the inside of the bean did not reach a high enough temperature to undergo the necessary reactions and produce satisfactory flavor. The roasts from the acidity control portion of this study can be used in a similar manner (Figure 3.4). The line through the faster roasts is higher than the line for the slower roasts, meaning that the inside of the bean is less roasted than the outside in faster roasting.

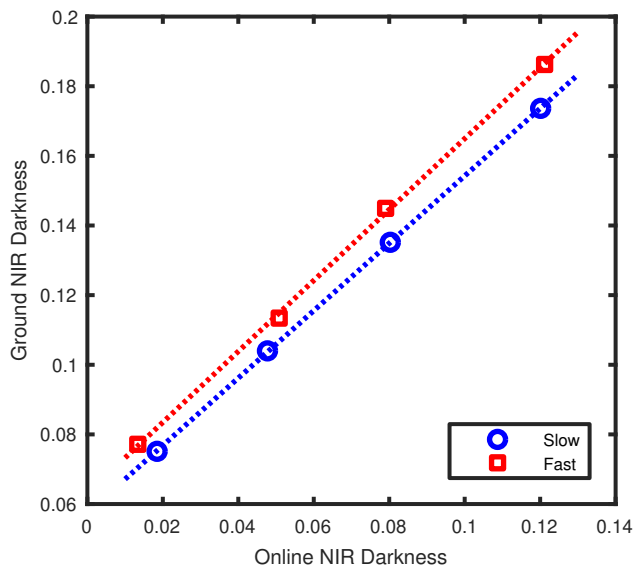


Figure 3.4: Comparing offline vs. ground NIR darkness correlation for high temperature fast roasts to low temperature slow roasts with separate trend lines (dotted).

3.4.4 Titratable Acidity Results

Titrateable acidity results (Appendix A), reported as the quantity of 0.1 M NaOH required to neutralize the acidity from 100 g of coffee, ranged from a maximum of nearly 200 mL to as low as 20 mL. The highest acidity occurred near the end of first crack, with the lowest values found at the darkest roasts. Slower, low-temperature roasting conditions also decreased the acidity in a given variety. In addition to differences caused by roasting, natural differences between coffees from different origins caused a high degree of variation in acidity. This is best observed based on differences in the peak acidity values measured for each variety, which varied from 146 to 199 mL 0.1 M NaOH/100 g. Scaling the acidity results by the maximum acidity observed for that coffee variety allowed this variation to be removed, emphasizing the differences caused by roasting. The researchers verified that several acidity values were measured near the peak of each variety to support the validity of the peak value, and subsequent conclusions were based on the set of eight varieties for statistical robustness. An example of the observed acidity values and scaled values is found in Figure 3.5.

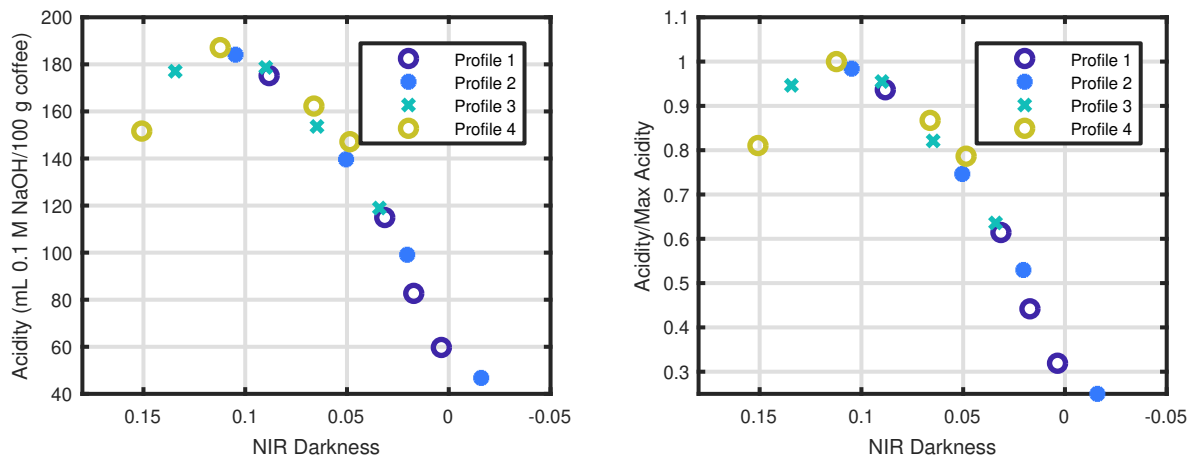


Figure 3.5: Measured and scaled acidity values vs NIR darkness for one coffee variety (Kenya).

3.4.5 Roast Scale Comparison

Results of the roast scale comparison by acidity (Figure 3.6) are split by roast profile because the different profiles are not expected to yield the same acidity trends. Samples from profiles 1 and 2 focused on acidity values after the peak acidity, so a decreasing trend is observed. Both the crack scale and NIR darkness scale show strong correlations to acidity measurements in the first two profiles, but more variation can be seen in the results on the visible lightness scale. Roast profiles 3 and 4 included some lighter samples removed before the peak acidity. In these roasts, the peak acidity location can be clearly seen and shows the least variation on the NIR darkness roast scale, especially in profile 4. The timing of this peak is especially important in light roasts, which are often valued for their high acidity [48].

Fitting each of these graphs with polynomial regression allowed a numerical comparison of the correlations (Table 3.1). These results come from first-order fits of roast profiles 1 and 2, which only contained samples after the peak acidity, and second-order fits of profiles 3 and 4. In all cases, the crack scale and NIR darkness result in better fit quality than visible lightness, and NIR darkness performs best in three of the four profiles. Therefore, the NIR darkness roast degree scale appears to be the best based on its strong correlation to coffee acidity.

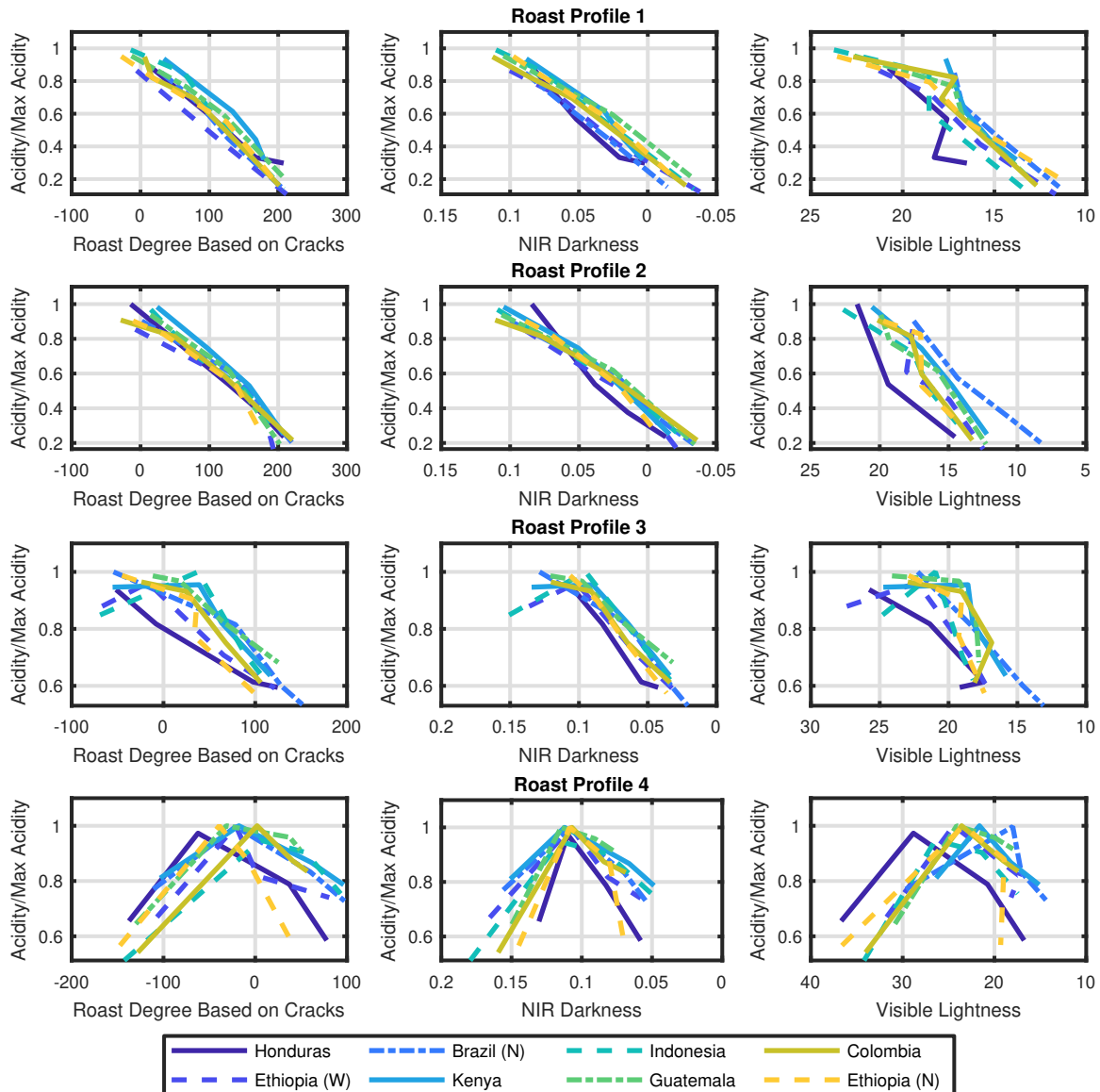


Figure 3.6: Comparing scaled titratable acidity values on three roast degree scales (columns 1-3), separated by roasting temperature profile (rows 1-4). Points from each roast are connected by lines representing eight coffee varieties.

The roast degree values at the start and end of the cracks can be used as another method of comparing roast degree scales, as these are already used as industry references. To determine the roast degree values at the crack events from ground coffee samples, the roast degree values were interpolated between the two samples nearest to the event. This method was used with NIR darkness as well as visible lightness. The results are displayed as box plots (Figure 3.7), where more separation can be seen between the NIR darkness results than visible lightness. It is especially important to be able to differentiate first crack end from second crack start, which separate light and

medium roasts, and second crack start from second crack end for dark roasts. Both of these ranges overlap in the visible lightness measurements, which again makes NIR darkness the better roast degree scale.

Table 3.1: Results of linear regression fits on the three roast degree scales vs. acidity. Root mean square error (RMSE) values are in terms of unit-less scaled acidity.

Profile	Crack Scale		NIR Darkness		Visible Lightness	
	R ²	RMSE	R ²	RMSE	R ²	RMSE
1	0.94	0.07	0.96	0.06	0.77	0.14
2	0.93	0.07	0.96	0.06	0.75	0.14
3	0.83	0.07	0.90	0.05	0.58	0.10
4	0.66	0.09	0.57	0.10	0.51	0.11

These box plots provide a reference for assigning the common light, medium, and dark roast ranges to the NIR darkness scale. The start of light roasting can be defined by the average location of peak acidity, which occurs before the average end of first crack. The transition to medium occurs between the crack events, and the transition to dark roast is often set at the start of second crack. Based on this, the range 0.12 to 0.08 would correspond to light roasting, 0.07 to 0.05 would be medium, and 0.04 and below would be dark.

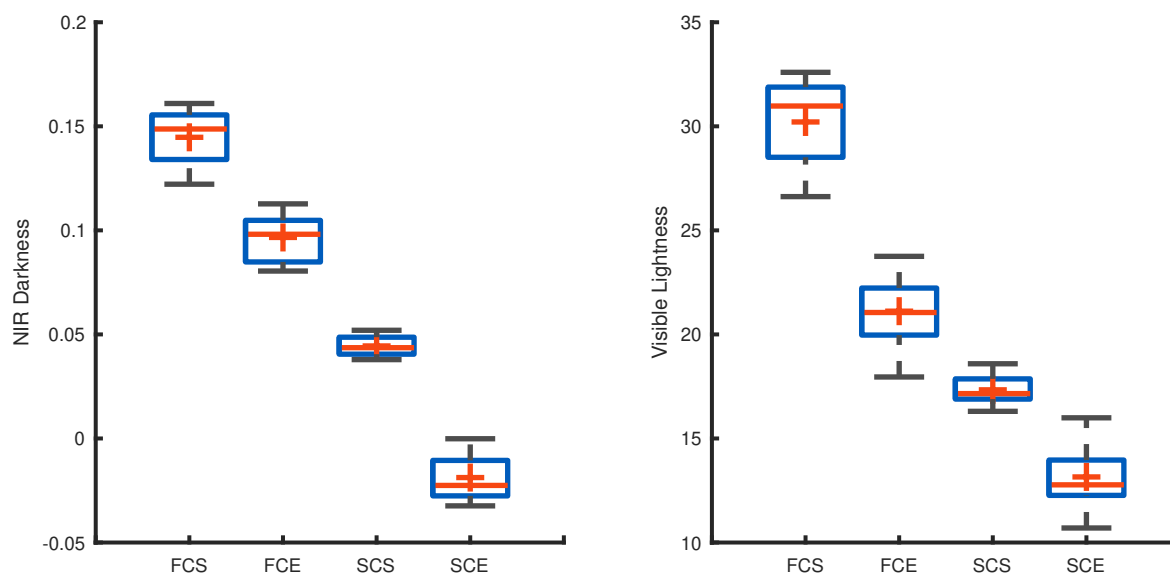


Figure 3.7: Box plots showing the roast degree values at first crack start (FCS), first crack end (FCE), second crack start (SCS), and second crack end (SCE) for NIR darkness and visible lightness roast degree scales.

3.4.6 Acidity Control Roast Profiles

A separate dataset, generated using constant inlet temperature roast profiles, demonstrates the ability to control acidity during roasting. The outlet air temperature during three sample roasts (Figure 3.8) provides insight into the coffee temperature relative to the inlet air temperature, showing that the coffee approaches the inlet air temperature in 300 s and surpasses the inlet temperature near 400 s due to exothermic roasting reactions. These times are related to the external heat transfer rate to the beans, which is determined by air velocity and mixing, and consequently, these inlet temperatures could not be applied to other roasters with the same results [17]. The more important aspect to focus on in the following results is the effect of changes in temperature on roast degree and acidity.

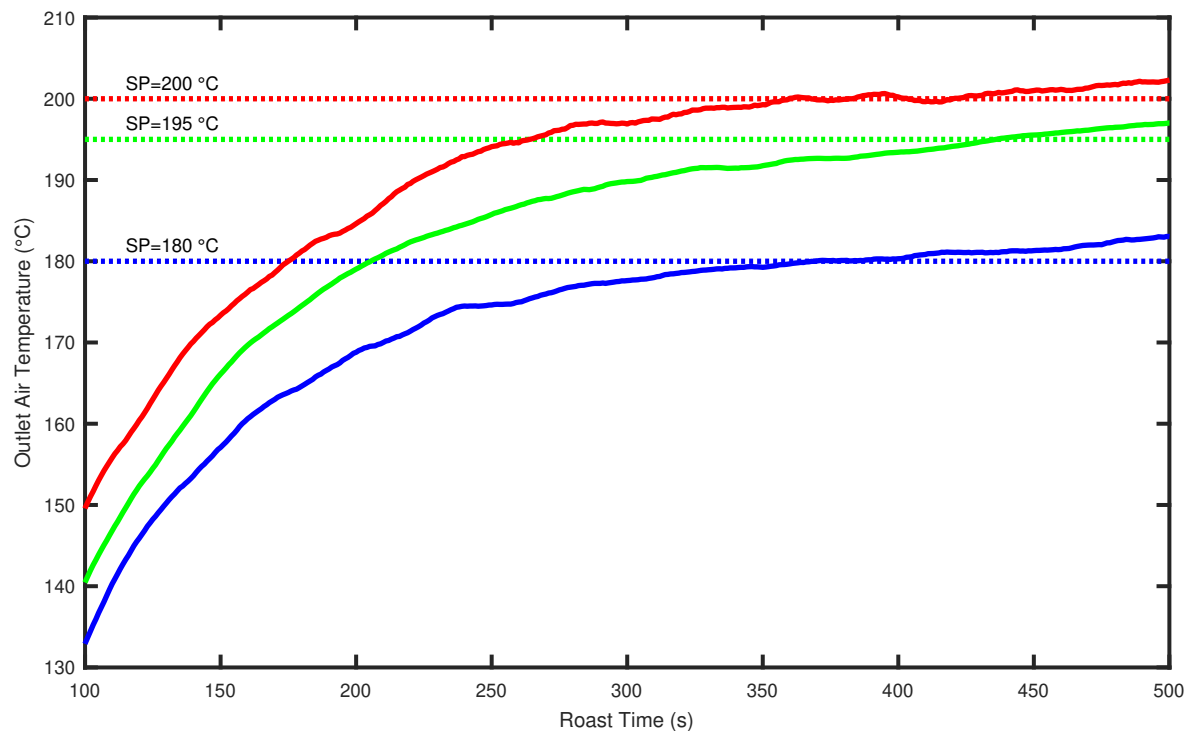


Figure 3.8: Outlet air temperatures (solid line) during the first 500 s of three constant inlet temperature roasts (dotted lines).

3.4.7 Acidity Control Roast Results

The results of the acidity control roasts (Figure 3.9) show the same acidity trends with respect to roast degree and roast profile as have been reported previously [30, 52, 58]. The slope of the lines demonstrates decreasing acidity at a constant roast degree as

the roast profile moves from high temperature-short duration to low temperature-long duration. Based on the slopes, the relationship does not appear to change drastically across roast degrees or coffee varieties. Acidity also decreases with increasing roast degree (smaller NIR darkness values), but the exact relationship is not clear based on this figure. Modeling these results helped to illustrate the relationships between four parameters (roast temperature, roast degree, time, acidity).

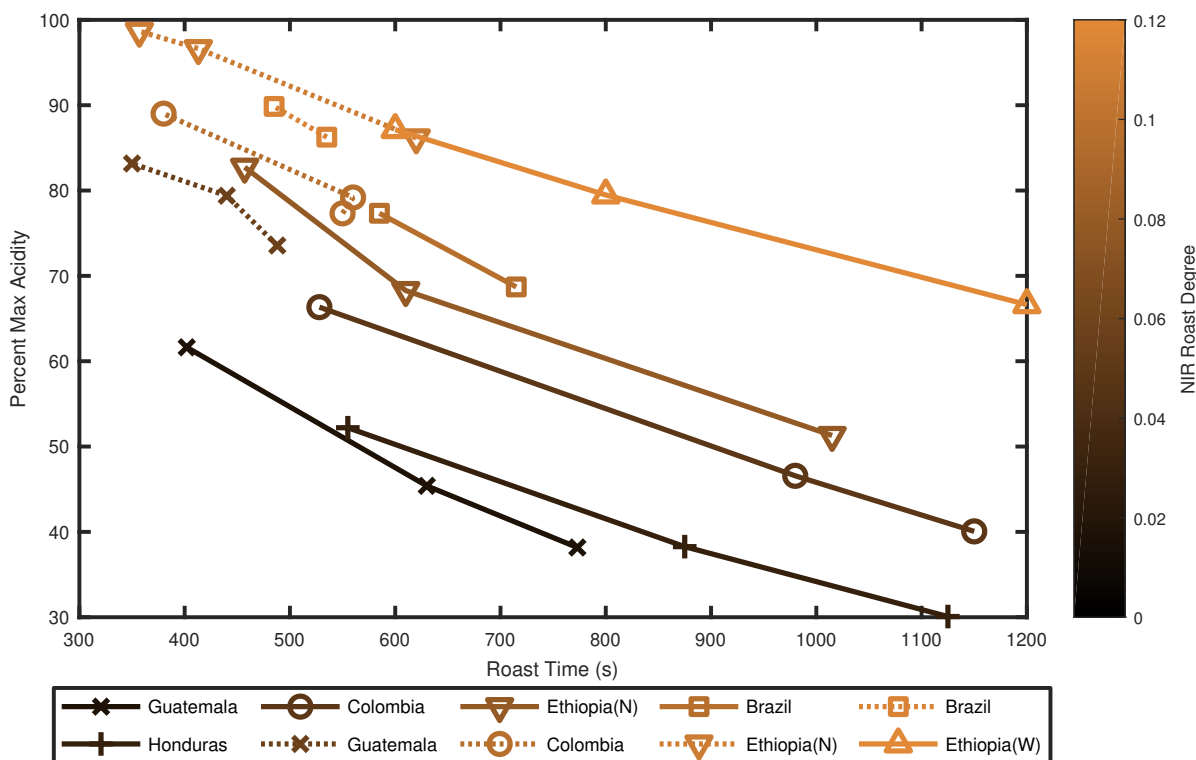


Figure 3.9: Constant temperature roast results for acidity control. Each line results from multiple roasts with the same coffee variety, to approximately the same NIR darkness roast degree, with different inlet air temperatures.

In Equation 3.1, scaled acidity is a linear function of roast degree (D) and time (t) in seconds, with an adjusted R² of 0.95. Plotting of the residuals by time (Figure 3.10a) showed a parabolic pattern, suggesting the possibility of a second-order relationship in time. The selected model did not include this second-order term, in favor of the simplicity found in a simple linear relationship that is independent of time and therefore has more significance to the non-constant roast temperature profiles typically used in industry. However, it is important to notice that the second-order term suggests a reduction in the rate of acidity decrease with increased roasting time. The residuals by roast degree (Figure 3.10b) show no pattern, indicating that the first-order fit in roast degree is sufficient.

$$Acidity = -0.0478t + 369D + 72.7 \quad (3.1)$$

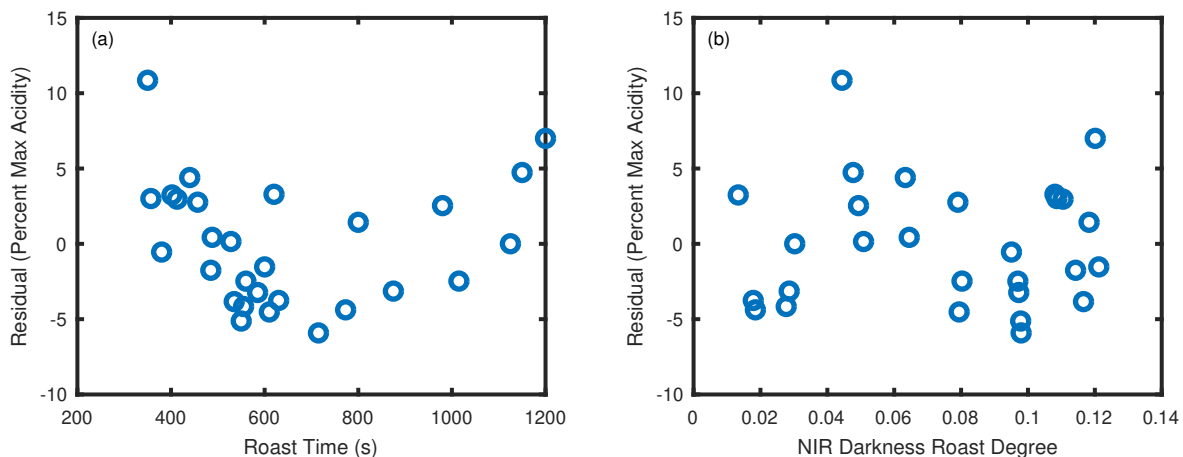


Figure 3.10: Residuals of the acidity model by time (a) and NIR darkness roast degree (b).

A second model shows the effect of time and temperature on roast degree. The trend observed in roast degree (Figure 3.11) during constant temperature roasts was a rapid initial decrease that levels off over time, which is not ideal for modeling with linear regression. The relationship resembles a first-order decay model, and because of its relevance to reaction kinetics, this became the basis of the nonlinear model. The exponential decay (Equation 3.2) moves from an initial roast degree (D_0) to a final roast degree (D_f) as a function of time (t) in seconds, but the final roast degree increased with temperature. Using the measured average of 0.33 for the initial roast degree and a linear relationship between final roast degree and time (Equation 3.3) resulted in three terms in the combined model, and solving this model with nonlinear regression in a standard error of 0.0095 NIR darkness units, with a range of 0.11 in the NIR darkness values and T in $^{\circ}\text{C}$.

$$D = D_f - (D_f - 0.33)e^{-0.00325t} \quad (3.2)$$

$$D_f = -0.00518T + 1.06 \quad (3.3)$$

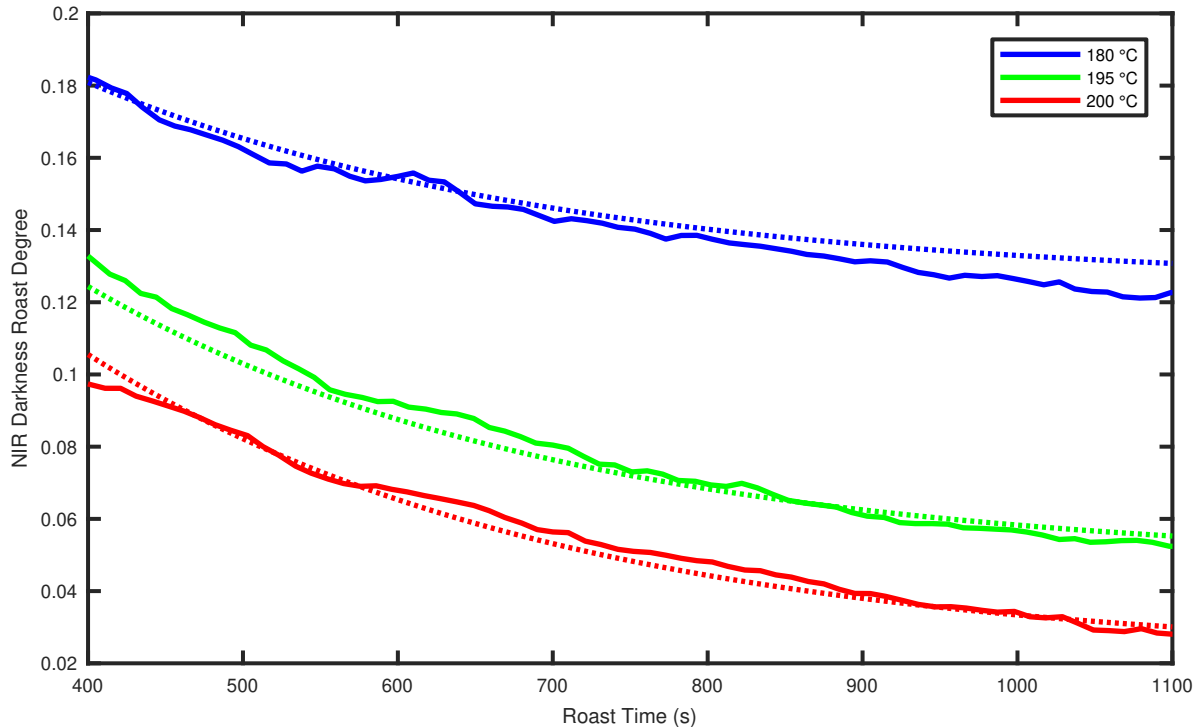


Figure 3.11: NIR darkness roast degree values observed in three example roasts (solid lines) with the modeled results (dotted lines).

These two models for acidity and roast degree allow the relationship between the four values to be viewed in a single plot (Figure 3.12), averaging differences between coffee varieties, deviation in the NIR spectra, and titratable acidity to demonstrate a simple relationship between the four values. This provides an indication of how changing the roast degree, temperature, and time affects acidity.

Both industrial and home roasting often take place in drum roasters, which have lower air velocities and require more time for the coffee to approach the inlet temperature. The temperature and time values from this study cannot be applied directly to these roasts. Instead, these relationships would be most valid in predicting the effect of extending or shortening the final stage of the roast, when the coffee is near its final temperature. For example, the slope of acidity at constant roast degree shows that increasing the roast time by 5 minutes will decrease the acidity by about 14% of the peak acidity. A similar comparison can be made with roast degree, where the acidity from a light roast with NIR darkness of 0.10 to a medium roast at 0.06 will decrease by about 15% if the roast time is held constant.

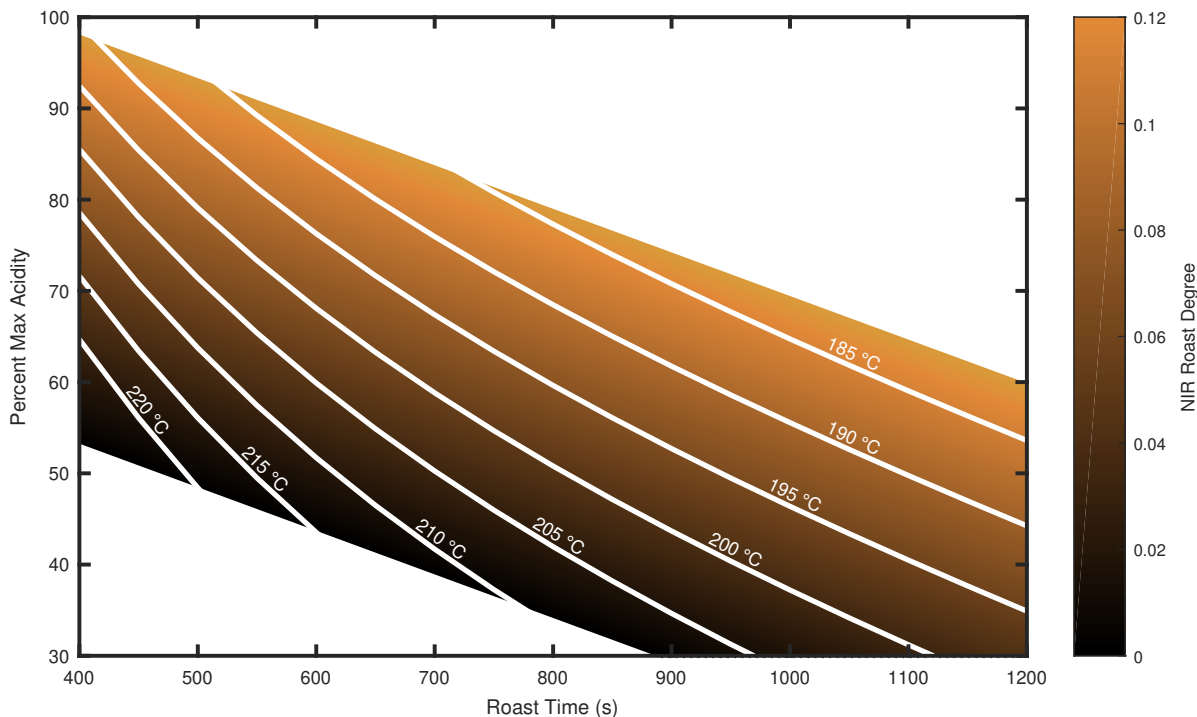


Figure 3.12: Relationship between acidity, roast time, roast degree (shown by color), and temperature (white lines) based on regression models for acidity and roast degree.

3.5 Conclusion

Comparing three roast degree scales based on their correlations to titratable acidity has shown that the NIR darkness and crack scales both correlate better to this property than visible lightness on the standard CIELAB color scale. NIR darkness performed best overall, and the greater simplicity of this scale makes it the recommended candidate for measuring roast degree, especially for future studies on other coffee properties. Measuring titratable acidity over a wide array of roast temperatures and times and then modeling the result allowed quantification of the relationships between acidity, roast time, and roast degree. Additional work to extend these results to other coffee attributes such as body, sweetness, aroma, or bitterness will help in developing a more complete understanding of the ability to target and control coffee flavors through the roast and lead to a roast degree scaling methodology with greater and more robust degrees of freedom for coffee attribute prediction and production.

CHAPTER 4 Conclusion and Recommendations

The results of this project show how NIR can be a useful tool for coffee roasting, providing real time feedback on roast degree to improve the roaster's ability to achieve a consistent result, and providing a reference for controlling coffee acidity independent of roast degree.

The use of recorded audio to determine crack times during roasting could be a useful, low cost tool for home roasters, removing some doubt as to when a past crack event started, reached a peak frequency, and ended. Predicting the start and end of these events with NIR spectroscopy and displaying the results in a new roast scale removes even more of the uncertainty in determining roast degree based on the cracks, providing a numerical scale which can be used to consistently achieve the same roast degree.

A new method for comparing roast degree scales based on measurements of important sensory attributes allowed the new crack scale to be compared to two other scales, with titratable acidity as a basis for comparison. This provided some validity to claims that visible color has shortcomings for measuring roast degree and showed that NIR measurements are more strongly tied to coffee acidity than visible lightness. Overall, the simple scale based on NIR absorbance from two wavelength ranges, called NIR darkness, performed best based on its strong tie to the peak acidity location. This roast scale does not require the hundreds of wavelengths provided by an NIR spectrometer and could potentially be measured by a lower cost sensor accessible to small industrial roasters or even home roasters.

The recommended NIR darkness sensor design uses two single-wavelength LEDs at 1350 and 1550 nm (7407 and 6452 cm^{-1}), have a reported wavelength range of 100 nm around the reported center, which is similar to the range used in developing the NIR darkness scale. The sensor would operate by turning on one set of LEDs, measuring the reflectance with the InGaAs photodiode, and then switching to the other set of LEDs and reading the reflectance again. This cycle could be repeated multiple times per second, depending on the response time of the LEDs and photodiode. The background signal due primarily to direct reflectance off of the glass roasting chamber

should be measured by reading the signal of both LED colors with the roasting chamber empty, providing a reference for 0% diffuse reflectance. The maximum reflectance should be measured by placing a piece of Teflon inside the roasting chamber and reading the two signals again as 100% diffuse reflectance. Finally, the reflectance values would be converted to absorbance and then subtracted from each other to produce the NIR darkness output.

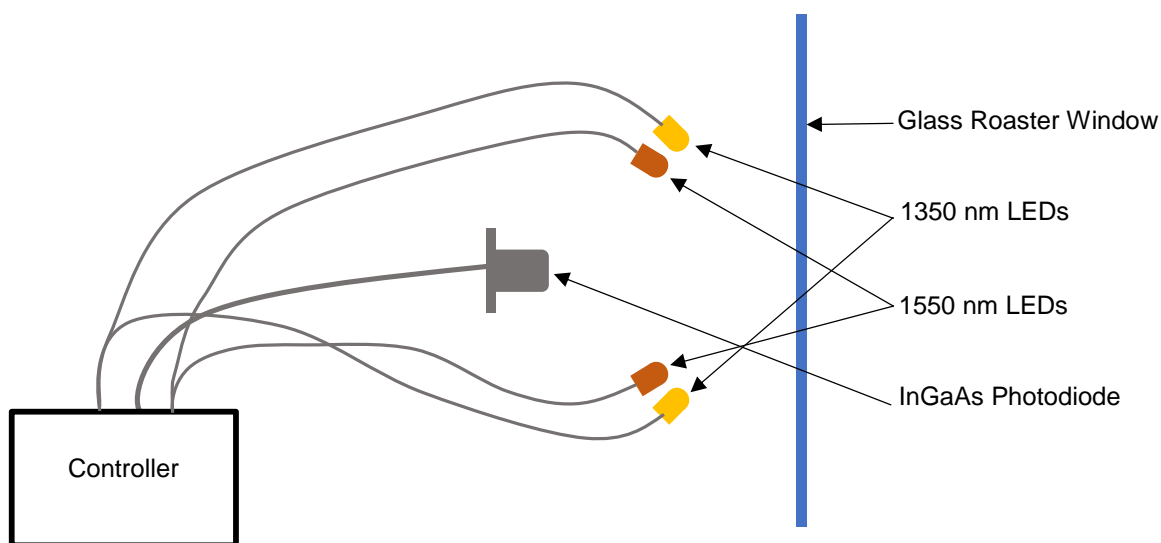


Figure 4.1: Design of a simple NIR darkness sensor.

Many NIR studies focus on directly measuring coffee aspects with NIR, and this would provide another valuable online roasting tool. Applying PLS regression to the acidity data from this study demonstrated this possibility and also showed the ability of the PLS model to respond to the acidity differences between different temperature profiles to the same roast degree (Appendix G).

The real time feedback provided by NIR darkness facilitated the measurement of simple numerical relationships describing the effects of roast degree and roast time on acidity during constant temperature roasts. This shows how roasters can control acidity by changing the roast temperature profile.

Future work could include extending these methods to other flavor characteristics for a more complete understanding of how coffee can be controlled by roasting. The ability to measure body in coffee would be especially useful in strengthening the roast scale comparison because increased body is an important characteristic of dark roasts. During the current project, tests to determine whether contact angle is related to body in coffee did not reveal a significant relationship, and neither did turbidity or

viscosity (Appendix F). Dissolved oils in brewed coffee and tannins are two additional measurements which may be worth exploring for their relation to body.

Body or another coffee attribute could be measured and used to compare roast scales in a similar analysis to section 3.4.5. If the new analysis results in the same conclusion, this would strengthen the comparison between NIR and visible roast degree, especially in dark roasts. If the results do not show the same conclusion, it may still be possible to modify the NIR roast scale to use different wavelengths that correlate well to both attributes. Additionally, a new measured attribute could be used to develop models similar to those in section 3.4.7, which shows the relationship between acidity, roast degree, temperature, and roast time. The new relationship may show a different correlation with other attributes than these, in which case the model may take a different form. For example, in the case of sucrose, a previous study suggested that sucrose is highly affected by the coffee temperature [53]. In this case, it may be best to model sucrose as a function of temperature instead of time. Determining the response of multiple attributes to different roasting conditions would create a new opportunity to control different combinations of these attributes (e.g. roast degree, acidity, and body) relative to each other using roast temperature profiles, which would provide an exciting new tool to enhance the art of coffee roasting.

References

- [1] AACC. “Near-Infrared Methods—Guidelines for Model Development and Maintenance”. In: *AACC International approved methods of analysis*. AACC International, 1999. Chap. 39-00.01.
- [2] Laura Alessandrini et al. “Near infrared spectroscopy: An analytical tool to predict coffee roasting degree”. In: *Analytica Chimica Acta* 625.1 (2008), pp. 95–102. ISSN: 0003-2670.
- [3] B. Anzueto et al. “The Plant”. In: *Espresso Coffee: The Science of Quality*. Ed. by A. Illy and R. Viani. Elsevier Academic, 2005. Chap. 2. ISBN: 9780123703712.
- [4] Association of Official Analytical Chemists AOAC. *Official Methods of Analysis of AOAC INTERNATIONAL*. 16th ed. Gaithersburg, MD, USA: AOAC International, 2005.
- [5] Juerg Baggenstoss et al. “Coffee roasting and aroma formation: application of different time-temperature conditions”. In: *Journal of Agricultural and Food Chemistry* 56.14 (2008), pp. 5836–5846.
- [6] H.H. Balzer. “Acids in Coffee”. In: *Coffee: Recent Developments*. Ed. by Ronald Clarke and O.G. Vitzthum. John Wiley & Sons, 2008. Chap. 1B.
- [7] D. F. Barbin et al. “Application of infrared spectral techniques on quality and compositional attributes of coffee: An overview”. In: *Food Research International* 61 (2014), pp. 23–32. ISSN: 0963-9969. DOI: 10.1016/j.foodres.2014.01.005.
- [8] S. Bee et al. “The raw bean”. In: *Espresso Coffee: The Science of Quality*. Ed. by A. Illy and R. Viani. Elsevier Academic, 2005. Chap. 3. ISBN: 9780123703712.
- [9] Elisa Bertone et al. “Simultaneous determination by NIR spectroscopy of the roasting degree and Arabica/Robusta ratio in roasted and ground coffee”. In: *Food Control* 59 (2016), pp. 683–689. ISSN: 0956-7135.
- [10] B. Bonnländer, R. Eggers, and H.G. Maier. “Roasting”. In: *Espresso Coffee: The Science of Quality*. Ed. by A. Illy and R. Viani. Elsevier Academic, 2005. Chap. 4. ISBN: 9780123703712.

- [11] *Brewing – the European Standard*. URL: <https://www.mountaincity.com/brewing-2.html>. Web Page. 2018.
- [12] Roberto A Buffo and Claudio Cardelli-Freire. “Coffee flavour: an overview”. In: *Flavour and fragrance journal* 19.2 (2004), pp. 99–104.
- [13] Nicola Caporaso et al. “Non-destructive analysis of sucrose, caffeine and trigonelline on single green coffee beans by hyperspectral imaging”. In: *Food Research International* 106 (2018), pp. 193–203. ISSN: 0963-9969.
- [14] Nicola Caporaso et al. “Rapid prediction of single green coffee bean moisture and lipid content by hyperspectral imaging”. In: *Journal of food engineering* 227 (2018), pp. 18–29. ISSN: 0260-8774.
- [15] Tiago A. Catelani et al. “A Non-invasive Real-Time Methodology for the Quantification of Antioxidant Properties in Coffee During the Roasting Process Based on Near-Infrared Spectroscopy”. In: *Food and Bioprocess Technology* 10.4 (2017), pp. 630–638. ISSN: 1935-5149. DOI: 10.1007/s11947-016-1843-6. URL: <https://doi.org/10.1007/s11947-016-1843-6>.
- [16] Tiago A Catelani et al. “Real-time monitoring of a coffee roasting process with near infrared spectroscopy using multivariate statistical analysis: A feasibility study”. In: *Talanta* 179 (2018), pp. 292–299. ISSN: 0039-9140.
- [17] Chao-Ching Chiang, Dai-Yuan Wu, and Dun-Yen Kang. “Detailed Simulation of Fluid Dynamics and Heat Transfer in Coffee Bean Roaster”. In: *Journal of food process engineering* 40.2 (2017), e12398.
- [18] Bingquan Chu et al. “Development of Noninvasive Classification Methods for Different Roasting Degrees of Coffee Beans Using Hyperspectral Imaging”. In: *Sensors* 18.4 (2018), p. 1259.
- [19] Ronald Clarke and OG Vitzthum. *Coffee: recent developments*. John Wiley & Sons, 2008.
- [20] Hendryk Czech et al. “Resolving coffee roasting-degree phases based on the analysis of volatile compounds in the roasting off-gas by photoionization time-of-flight mass spectrometry (PI-TOFMS) and statistical data analysis: toward a PI-TOFMS roasting model”. In: *Journal of agricultural and food chemistry* 64.25 (2016), pp. 5223–5231.
- [21] Edith Ramos Da Conceicao Neta, Suzanne D Johanningsmeier, and Roger F McFeeters. “The chemistry and physiology of sour taste—a review”. In: *Journal of food science* 72.2 (2007), R33–R38.

- [22] Kenneth Davids. *Home Coffee Roasting, Revised, Updated Edition: Romance and Revival*. Macmillan, 2003.
- [23] Ralph Dorfner et al. "Laser mass spectrometry as on-line sensor for industrial process analysis: process control of coffee roasting". In: *Analytical Chemistry* 76.5 (2004), pp. 1386–1402.
- [24] Ralph Dorfner et al. "Real-time monitoring of 4-vinylguaiacol, guaiacol, and phenol during coffee roasting by resonant laser ionization time-of-flight mass spectrometry". In: *Journal of Agricultural and Food Chemistry* 51.19 (2003), pp. 5768–5773.
- [25] I Esteban-Díez, JM González-Sáiz, and C Pizarro. "Prediction of roasting colour and other quality parameters of roasted coffee samples by near infrared spectroscopy. A feasibility study". In: *Journal of near infrared spectroscopy* 12.5 (2004), pp. 287–297. ISSN: 1751-6552.
- [26] I Esteban-Díez, JM González-Sáiz, and C Pizarro. "Prediction of sensory properties of espresso from roasted coffee samples by near-infrared spectroscopy". In: *Analytica Chimica Acta* 525.2 (2004a), pp. 171–182. ISSN: 0003-2670.
- [27] Suzana Reis Evangelista et al. "Improvement of coffee beverage quality by using selected yeasts strains during the fermentation in dry process". In: *Food Research International* 61 (2014). Coffee – Science, Technology and Impacts on Human Health, pp. 183–195. ISSN: 0963-9969. DOI: <https://doi.org/10.1016/j.foodres.2013.11.033>. URL: <http://www.sciencedirect.com/science/article/pii/S096399691300642X>.
- [28] N. T. Fadaei et al. "A heat and mass transfer study of coffee bean roasting". In: *International Journal of Heat and Mass Transfer* 104 (2017), pp. 787–799. ISSN: 0017-9310. DOI: [10.1016/j.ijheatmasstransfer.2016.08.083](https://doi.org/10.1016/j.ijheatmasstransfer.2016.08.083).
- [29] Adriana S. Franca et al. "A preliminary evaluation of the effect of processing temperature on coffee roasting degree assessment". In: *Journal of Food Engineering* 92.3 (2009), pp. 345–352. ISSN: 0260-8774. DOI: <https://doi.org/10.1016/j.jfoodeng.2008.12.012>. URL: <http://www.sciencedirect.com/science/article/pii/S026087740800589X>.
- [30] Alexia N Gloess et al. "Evidence of different flavour formation dynamics by roasting coffee from different origins: On-line analysis with PTR-ToF-MS". In: *International Journal of Mass Spectrometry* 365 (2014), pp. 324–337.

- [31] *Guidelines for Using By-Pass in the Drip Coffee Brewing Process*. Web Page. 2016. URL: <https://www.scaa.org/PDF/resources/best-practices-bypass-brewing.pdf>.
- [32] Molly J Hall et al. "PTC taste blindness and the taste of caffeine". In: *Nature* 253.5491 (1975), p. 442.
- [33] Romy Hertz-Schünemann et al. "Looking into individual coffee beans during the roasting process: direct micro-probe sampling on-line photo-ionisation mass spectrometric analysis of coffee roasting gases". In: *Analytical and Bioanalytical Chemistry* 405.22 (2013), pp. 7083–7096. ISSN: 1618-2650. DOI: 10.1007/s00216-013-7006-y. URL: <https://doi.org/10.1007/s00216-013-7006-y>.
- [34] Romy Hertz-Schünemann et al. "On-line process monitoring of coffee roasting by resonant laser ionisation time-of-flight mass spectrometry: bridging the gap from industrial batch roasting to flavour formation inside an individual coffee bean". In: *Journal of Mass Spectrometry* 48.12 (2013), pp. 1253–1265.
- [35] ICO. *Annual Review 2016/17*. London, UK: International Coffee Organization, 2017.
- [36] International Commission on Illumination. *Colorimetry*. Commission internationale de l'Eclairage, CIE Central Bureau, 2004. ISBN: 9783901906336. URL: <https://books.google.com/books?id=P1NkAAAACAAJ>.
- [37] A. Illy and R. Viani. *Espresso Coffee: The Science of Quality*. Elsevier Academic, 2005. ISBN: 9780123703712.
- [38] ITC. *The Coffee Exporter's Guide*. 3rd ed. Geneva, Switzerland: International Trade Centre, 2011. ISBN: 978-92-9137-394-9.
- [39] Hong-Dong Li, Qing-Song Xu, and Yi-Zeng Liang. "libPLS: An integrated library for partial least squares regression and linear discriminant analysis". In: *Chemo-metrics and Intelligent Laboratory Systems* 176 (2018), pp. 34–43. ISSN: 0169-7439.
- [40] Erica Liberto et al. "Non-separative headspace solid phase microextraction–mass spectrometry profile as a marker to monitor coffee roasting degree". In: *Journal of agricultural and food chemistry* 61.8 (2012), pp. 1652–1660.
- [41] Gilberto Vinícius de Melo Pereira et al. "Isolation, selection and evaluation of yeasts for use in fermentation of coffee beans by the wet process". In: *International journal of food microbiology* 188 (2014), pp. 60–66.

- [42] Joon-Kwan Moon, Hyui Sun Yoo, and Takayuki Shibamoto. "Role of roasting conditions in the level of chlorogenic acid content in coffee beans: correlation with coffee acidity". In: *Journal of agricultural and food chemistry* 57.12 (2009), pp. 5365–5369.
- [43] Yukihiro Ozaki, W Fred McClure, and Alfred A Christy. *Near-infrared spectroscopy in food science and technology*. John Wiley & Sons, 2006.
- [44] Catarina Petisca et al. "Furans and other volatile compounds in ground roasted and espresso coffee using headspace solid-phase microextraction: Effect of roasting speed". In: *Food and Bioproducts Processing* 91.3 (2013), pp. 233–241.
- [45] M. Petracco. "Grinding". In: *Espresso Coffee: The Science of Quality*. Ed. by A. Illy and R. Viani. Elsevier Academic, 2005. Chap. 5. ISBN: 9780123703712.
- [46] D. Pramudita et al. "Roasting and Colouring Curves for Coffee Beans with Broad Time-Temperature Variations". In: *Food and Bioprocess Technology* 10.8 (2017), pp. 1509–1520. ISSN: 1935-5149. DOI: 10.1007/s11947-017-1912-5. URL: <https://doi.org/10.1007/s11947-017-1912-5>.
- [47] *Protocols & Best Practices*. Web Page. 2017. URL: <https://sca.coffee/research/protocols-best-practices>.
- [48] Scott Rao. *The Coffee Roaster's Companion*. Ed. by Scott Rao. Scott Rao, 2014. ISBN: 978-1-4951-1819-7.
- [49] JS Ribeiro, MMC Ferreira, and TJG Salva. "Chemometric models for the quantitative descriptive sensory analysis of Arabica coffee beverages using near infrared spectroscopy". In: *Talanta* 83.5 (2011), pp. 1352–1358. ISSN: 0039-9140.
- [50] Luciana Silva Ribeiro et al. "Behavior of yeast inoculated during semi-dry coffee fermentation and the effect on chemical and sensorial properties of the final beverage". In: *Food Research International* 92 (2017), pp. 26–32. ISSN: 0963-9969. DOI: <https://doi.org/10.1016/j.foodres.2016.12.011>. URL: <http://www.sciencedirect.com/science/article/pii/S0963996916306056>.
- [51] Saskia M van Ruth. "Methods for gas chromatography-olfactometry: a review". In: *Biomolecular Engineering* 17.4 (2001), pp. 121–128. ISSN: 1389-0344. DOI: [https://doi.org/10.1016/S1389-0344\(01\)00070-3](https://doi.org/10.1016/S1389-0344(01)00070-3). URL: <http://www.sciencedirect.com/science/article/pii/S1389034401000703>.

- [52] J. R. Santos et al. "Exploiting near infrared spectroscopy as an analytical tool for on-line monitoring of acidity during coffee roasting". In: *Food Control* 60 (2016), pp. 408–415. ISSN: 0956-7135. DOI: 10.1016/j.foodcont.2015.08.007.
- [53] J. R. Santos et al. "In-line monitoring of the coffee roasting process with near infrared spectroscopy: Measurement of sucrose and colour". In: *Food Chemistry* 208 (2016), pp. 103–110. ISSN: 0308-8146. DOI: 10.1016/j.foodchem.2016.03.114.
- [54] Abraham Savitzky and Marcel JE Golay. "Smoothing and differentiation of data by simplified least squares procedures." In: *Analytical chemistry* 36.8 (1964), pp. 1627–1639.
- [55] S Schenker et al. "Impact of roasting conditions on the formation of aroma compounds in coffee beans". In: *Journal of food science* 67.1 (2002), pp. 60–66.
- [56] Lucia Solis. Web Page. 2017. URL: <https://www.scottrao.com/blog/2017/10/23/looking-beyond-origin-for-flavor-diversity>.
- [57] W. B. Sunarharum, D. J. Williams, and H. E. Smyth. "Complexity of coffee flavor: A compositional and sensory perspective". In: *Food Research International* 62 (2014), pp. 315–325. ISSN: 0963-9969. DOI: 10.1016/j.foodres.2014.02.030.
- [58] Niya Wang and Loong-Tak Lim. "Fourier transform infrared and physicochemical analyses of roasted coffee". In: *Journal of agricultural and food chemistry* 60.21 (2012), pp. 5446–5453.
- [59] He-Ya Wang, He Qian, and Wei-Rong Yao. "Melanoidins produced by the Maillard reaction: Structure and biological activity". In: *Food Chemistry* 128.3 (2011), pp. 573–584.
- [60] Flurin Wieland et al. "Online monitoring of coffee roasting by proton transfer reaction time-of-flight mass spectrometry (PTR-ToF-MS): towards a real-time process control for a consistent roast profile". In: *Analytical and bioanalytical chemistry* 402.8 (2012), pp. 2531–2543.
- [61] Preston S. Wilson. "Coffee roasting acoustics". In: *The Journal of the Acoustical Society of America* 135.6 (2014), EL265–EL269. DOI: 10.1121/1.4874355. URL: <https://asa.scitation.org/doi/abs/10.1121/1.4874355>.
- [62] Fathurrozi Winjaya, Muhammad Rivai, and Djoko Purwanto. "Identification of cracking sound during coffee roasting using neural network". In: *Intelligent Technology and Its Applications (ISITIA), 2017 International Seminar on*. IEEE, pp. 271–274. ISBN: 1538627086.

APPENDIX A Roast Degree Acidity Data

Table A.1: Titratable acidity results for 32 roasts with 4 samples per roast. Used for comparing roast degree scales and to generate a PLS model based on acidity.

Sample	Variety	Roast Profile	Roast Time	Acidity (mL 0.1 M NaOH / 100 g coffee)	Online NIR Darkness	Visible Lightness	Crack Roast Degree
1	Honduran	1	520	129.1	0.084	20.8	16
2	Honduran	1	630	83.3	0.052	17.6	107
3	Honduran	1	755	48.7	0.021	18.3	167
4	Honduran	1	905	43.7	0.002	16.5	208
5	Honduran	2	490	146.7	0.084	21.6	-14
6	Honduran	2	595	78.9	0.038	19.4	128
7	Honduran	2	665	55.2	0.015	16.8	175
8	Honduran	2	750	34.4	-0.013	14.5	208
9	Honduran	3	425	137.6	0.104	25.8	-52
10	Honduran	3	505	119.9	0.083	21.4	-8
11	Honduran	3	585	90.0	0.055	17.5	98
12	Honduran	3	620	87.2	0.042	19.2	125
13	Honduran	4	380	96.1	0.131	36.7	-138
14	Honduran	4	455	142.8	0.110	28.8	-62
15	Honduran	4	537	115.6	0.083	20.8	37
16	Honduran	4	600	85.8	0.058	16.8	78
17	Ethiopian Washed	1	490	153.7	0.100	21.3	-6
18	Ethiopian Washed	1	595	127.5	0.066	18.4	35
19	Ethiopian Washed	1	750	73.7	0.022	15.8	122
20	Ethiopian Washed	1	1120	19.1	-0.041	11.7	212
21	Ethiopian Washed	2	485	152.0	0.090	17.6	-7
22	Ethiopian Washed	2	575	108.5	0.042	18.1	110
23	Ethiopian Washed	2	645	79.9	0.006	14.9	175

24	Ethiopian Washed	2	815	29.3	-0.021	12.5	193
25	Ethiopian Washed	3	395	156.4	0.136	27.4	-67
26	Ethiopian Washed	3	460	171.1	0.102	22.3	-17
27	Ethiopian Washed	3	555	125.9	0.058	18.5	66
28	Ethiopian Washed	3	610	105.2	0.032	17.2	121
29	Ethiopian Washed	4	395	119.1	0.166	31.7	-107
30	Ethiopian Washed	4	480	177.9	0.108	24.5	-21
31	Ethiopian Washed	4	545	145.5	0.082	17.3	3
32	Ethiopian Washed	4	585	131.7	0.058	18.2	81
33	Brazil Natural	1	520	136.4	0.089	17.2	31
34	Brazil Natural	1	620	104.6	0.060	16.8	87
35	Brazil Natural	1	715	72.0	0.029	14.7	127
36	Brazil Natural	1	914	24.4	-0.014	11.5	204
37	Brazil Natural	2	475	145.0	0.100	17.5	2
38	Brazil Natural	2	585	92.2	0.021	14.4	145
39	Brazil Natural	2	640	54.4	-0.008	10.5	190
40	Brazil Natural	2	700	31.0	-0.033	8.2	222
41	Brazil Natural	3	402	160.5	0.129	22.2	-54
42	Brazil Natural	3	494	130.9	0.064	18.4	78
43	Brazil Natural	3	542	96.4	0.033	14.6	128
44	Brazil Natural	3	570	85.1	0.021	13.1	153
45	Brazil Natural	4	385	123.7	0.156	29.7	-111
46	Brazil Natural	4	475	160.1	0.109	18.0	-21
47	Brazil Natural	4	540	133.7	0.070	17.1	60
48	Brazil Natural	4	568	116.8	0.054	14.3	97
49	Kenya	1	473	175.2	0.088	17.7	34
50	Kenya	1	605	114.9	0.031	16.6	134
51	Kenya	1	665	82.7	0.017	15.3	167
52	Kenya	1	721	59.7	0.004	13.8	179
53	Kenya	2	418	184.1	0.105	20.6	24
54	Kenya	2	515	139.6	0.050	17.0	97
55	Kenya	2	582	99.1	0.020	14.7	158
56	Kenya	2	688	46.8	-0.016	12.2	208
57	Kenya	3	385	177.1	0.134	24.7	-55
58	Kenya	3	461	178.7	0.090	18.6	39

59	Kenya	3	513	153.6	0.065	18.2	63
60	Kenya	3	560	119.0	0.034	15.8	117
61	Kenya	4	390	151.7	0.151	26.4	-104
62	Kenya	4	450	187.1	0.112	21.6	-18
63	Kenya	4	534	162.3	0.066	18.2	61
64	Kenya	4	560	147.1	0.049	15.1	96
65	Indonesia	1	433	186.1	0.110	23.7	-14
66	Indonesia	1	530	159.4	0.074	18.6	64
67	Indonesia	1	625	114.7	0.040	18.6	102
68	Indonesia	1	990	26.2	-0.033	13.4	208
69	Indonesia	2	435	181.9	0.109	22.7	15
70	Indonesia	2	535	134.7	0.057	17.6	75
71	Indonesia	2	615	94.7	0.015	16.4	152
72	Indonesia	2	705	49.0	-0.021	13.8	198
73	Indonesia	3	388	159.4	0.151	24.8	-69
74	Indonesia	3	465	187.8	0.095	21.0	37
75	Indonesia	3	565	132.5	0.048	19.0	90
76	Indonesia	3	595	116.7	0.034	18.2	111
77	Indonesia	4	360	96.2	0.179	34.2	-143
78	Indonesia	4	455	178.0	0.115	26.5	6
79	Indonesia	4	514	169.7	0.082	21.4	55
80	Indonesia	4	560	141.6	0.050	17.5	93
81	Guatemala	1	485	166.2	0.105	22.6	-13
82	Guatemala	1	600	133.5	0.063	17.2	66
83	Guatemala	1	695	103.6	0.026	16.8	121
84	Guatemala	1	957	37.8	-0.031	13.2	206
85	Guatemala	2	480	163.5	0.106	19.9	15
86	Guatemala	2	566	136.3	0.066	19.3	70
87	Guatemala	2	655	107.9	0.025	15.8	128
88	Guatemala	2	901	33.7	-0.034	12.3	202
89	Guatemala	3	455	171.9	0.121	24.1	-12
90	Guatemala	3	522	168.6	0.098	19.2	18
91	Guatemala	3	583	144.4	0.070	18.0	63
92	Guatemala	3	657	118.8	0.032	17.8	125
93	Guatemala	4	395	112.4	0.150	30.8	-130

94	Guatemala	4	480	174.3	0.115	24.1	-31
95	Guatemala	4	538	167.0	0.091	20.0	38
96	Guatemala	4	562	159.0	0.077	17.8	49
97	Colombia	1	470	188.4	0.113	22.7	6
98	Colombia	1	560	163.1	0.085	17.1	17
99	Colombia	1	635	137.7	0.055	17.9	78
100	Colombia	1	1111	31.9	-0.028	12.7	202
101	Colombia	2	465	180.4	0.111	20.2	-29
102	Colombia	2	550	161.7	0.077	17.7	49
103	Colombia	2	648	118.5	0.029	16.9	119
104	Colombia	2	889	42.9	-0.036	13.3	221
105	Colombia	3	445	191.6	0.120	23.0	-24
106	Colombia	3	520	185.0	0.091	19.1	25
107	Colombia	3	585	149.3	0.065	16.9	68
108	Colombia	3	650	121.4	0.034	18.1	106
109	Colombia	4	380	107.5	0.160	34.0	-128
110	Colombia	4	480	198.7	0.107	23.6	2
111	Colombia	4	533	173.6	0.084	19.1	41
112	Colombia	4	560	165.9	0.069	17.4	57
113	Ethiopian Natural	1	490	156.5	0.098	23.6	-28
114	Ethiopian Natural	1	585	130.5	0.070	18.5	28
115	Ethiopian Natural	1	713	90.8	0.025	16.5	125
116	Ethiopian Natural	1	935	33.6	-0.020	11.4	192
117	Ethiopian Natural	2	522	148.6	0.089	19.7	-11
118	Ethiopian Natural	2	576	135.9	0.071	17.0	34
119	Ethiopian Natural	2	711	87.0	0.021	17.0	139
120	Ethiopian Natural	2	836	48.2	-0.003	14.0	171
121	Ethiopian Natural	3	498	162.5	0.106	22.9	-45
122	Ethiopian Natural	3	580	147.8	0.087	19.1	36
123	Ethiopian Natural	3	640	127.4	0.069	19.3	34
124	Ethiopian Natural	3	730	94.6	0.036	17.4	99
125	Ethiopian Natural	4	405	93.2	0.145	36.6	-147
126	Ethiopian Natural	4	535	164.6	0.109	23.4	-39
127	Ethiopian Natural	4	615	144.6	0.080	18.9	-9
128	Ethiopian Natural	4	660	93.6	0.070	19.3	41

APPENDIX B Crack Data

Table B.1: Crack start and end times determined by recorded audio from 32 roasts with 8 coffee varieties and 4 roast temperature profiles.

Variety	Roast Profile	First Crack Start (s)	First Crack End (s)	Second Crack Start (s)	Second Crack End (s)
Honduran	1	386	529	594	860
Honduran	2	371	504	572	711
Honduran	3	0	520	586	0
Honduran	4	422	539	0	0
Ethiopian Washed	1	349	521	680	1092
Ethiopian Washed	2	342	482	566	771
Ethiopian Washed	3	349	512	601	0
Ethiopian Washed	4	387	516	0	0
Brazil Natural	1	388	456	651	0
Brazil Natural	2	389	474	532	670
Brazil Natural	3	373	426	520	0
Brazil Natural	4	396	499	0	0
Kenya	1	346	412	562	689
Kenya	2	335	415	518	659
Kenya	3	341	414	551	0
Kenya	4	384	463	0	0
Indonesia	1	370	405	619	949
Indonesia	2	354	416	566	687

Indonesia	3	340	409	587	0
Indonesia	4	372	419	0	0
Guatemala	1	371	506	637	926
Guatemala	2	382	459	602	858
Guatemala	3	395	469	643	0
Guatemala	4	417	486	0	0
Colombia	1	357	466	669	1084
Colombia	2	364	478	607	858
Colombia	3	384	466	641	0
Colombia	4	403	509	0	0
Ethiopian Natural	1	379	540	661	897
Ethiopian Natural	2	407	588	652	818
Ethiopian Natural	3	424	541	726	0
Ethiopian Natural	4	464	587	0	0

APPENDIX C Crack PLS Coefficients

PLS models consist of a matrix of coefficients which are multiplied by the matrix of predictor variables to determine the response variable. These predictors indicate the effect each wavelength has on the output and can be used to determine the most important regions of the spectrum for a given model. A higher the coefficient magnitude signifies a higher influence for that predictor, but if the value of the predictor does not change between different data points, the influence of that predictor will be low independent of the coefficient value. To account for this, the coefficients can be multiplied by the standard deviation of the corresponding predictor value to generate an importance value for each wavelength (Figure C.1).

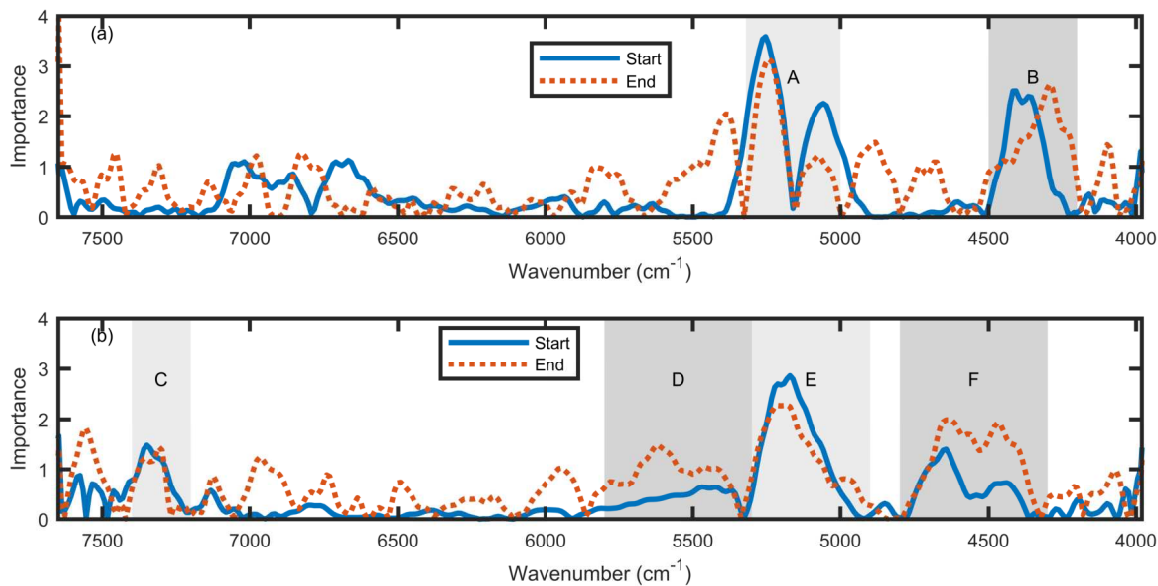


Figure C.1: Absolute value of the PLS predictor importance in the models for first crack (a) and second crack (b) with the most important regions labeled A-F. Results have been smoothed to improve readability.

APPENDIX D Scaled Acidity Plots

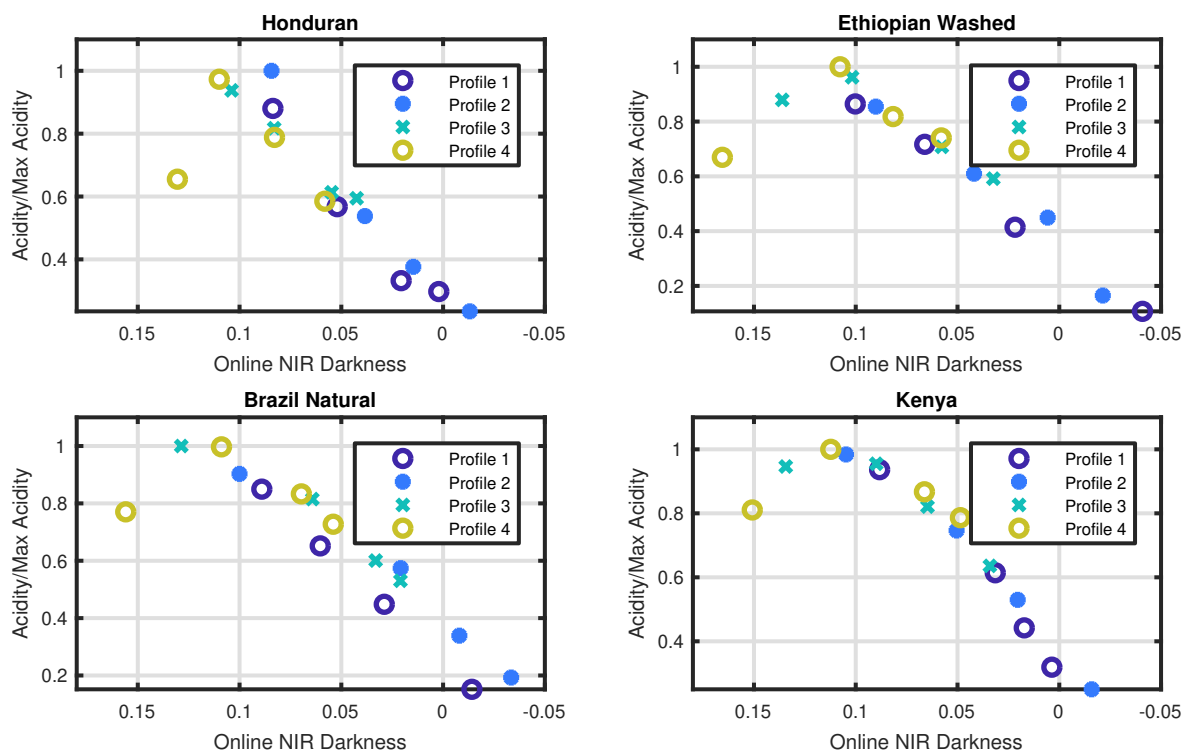


Figure D.1: Acidity scaled by the maximum acidity measured. First 4 varieties.

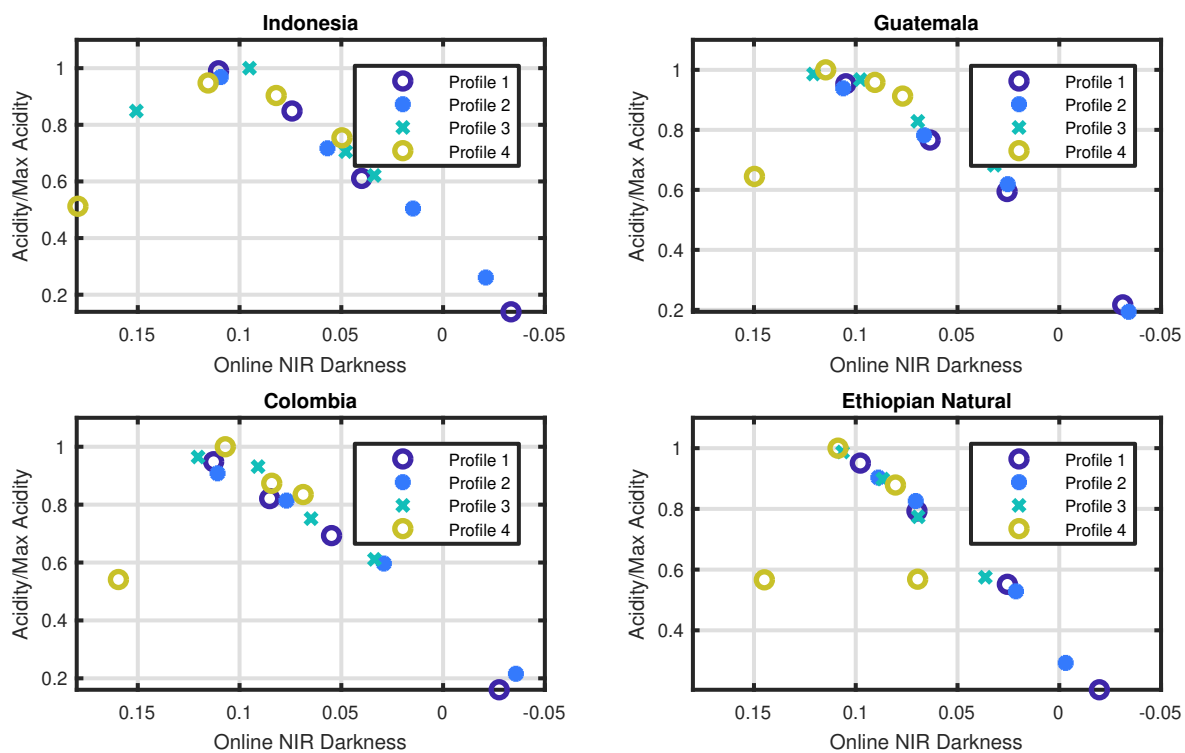


Figure D.2: Acidity scaled by the maximum acidity measured. Last 4 varieties.

APPENDIX E Acidity Control Data

Table E.1: Data from constant temperature roast profiles for acidity control described in Chapter 3

Variety	Roast Temperature (°C)	Roast Time (s)	Relative Acidity (%)	Online NIR Darkness	Ground NIR Darkness
Colombia	195	550	77.3	0.098	0.152
Colombia	195	1150	40.1	0.048	0.104
Colombia	200	560	79.2	0.097	0.159
Colombia	200	980	46.6	0.049	0.106
Colombia	205	380	89.0	0.095	0.166
Colombia	205	528	66.3	0.051	0.113
Guatemala	204	488	73.6	0.064	0.128
Guatemala	204	773	38.2	0.018	0.075
Guatemala	208	440	79.4	0.063	0.134
Guatemala	208	630	45.4	0.018	0.071
Guatemala	220	350	83.2	0.044	0.117
Guatemala	220	402	61.6	0.013	0.077
Ethiopia Washed	180	1200	66.6	0.120	0.174
Ethiopia Washed	185	800	79.5	0.118	0.177
Ethiopia Washed	190	600	87.1	0.121	0.186
Ethiopia Natural	190	620	86.2	0.108	0.165
Ethiopia Natural	190	1015	51.3	0.080	0.135
Ethiopia Natural	198	413	96.6	0.110	0.173

Ethiopia Natural	198	610	68.3	0.079	0.141
Ethiopia Natural	205	357	98.7	0.109	0.166
Ethiopia Natural	205	457	82.7	0.079	0.145
Brazil Natural	187	535	86.3	0.117	0.166
Brazil Natural	187	715	68.7	0.098	0.147
Brazil Natural	194	485	89.9	0.114	0.165
Brazil Natural	194	585	77.3	0.097	0.152
Honduras	200	1125	30.1	0.030	0.085
Honduras	203	875	38.3	0.029	0.086
Honduras	210	555	52.2	0.028	0.085

APPENDIX F Coffee Body Measurement Attempts

F.1 Contact Angle

These experiments attempted to determine whether contact angle can be used to measure body in coffee. The perceived body of coffee increases with roast extent and this is often associated with the amount of oil dissolved in the coffee. The research question here was whether changes in contact angle are related to the amount of oil dissolved in brewed coffee and consequently, body. The oils may act as surfactants on the surface of the droplet, reducing the surface tension and decreasing the contact angle.

A goniometer read contact angles of droplets placed on a thin glass slide coated with Rain-X®. The slide was placed on a heated aluminum block for temperature control. Contact angles were measured on the right and left edge of 10-20 droplets, and this was repeated for three roast degrees on the same batch of brewed coffee. This test showed an increasing trend in the contact angle with roast extent, which is opposite to the expected trend, bringing the contact angle closer to that of pure water (104°).

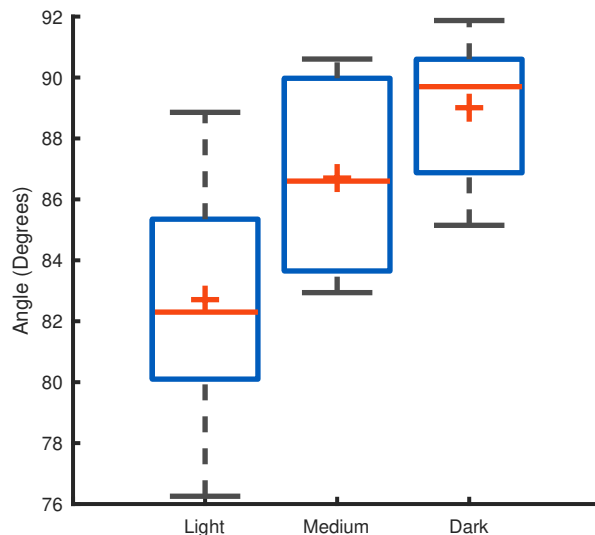


Figure F.1: Contact angle on Rain-X® coated slides on an aluminum block heated to 70 °C.

The same test performed with the coffee in a boiling water bath to keep it from cooling before removing samples no longer showed the upward trend as the roast degree increased, but there was not a significant difference between the means. It is possible that the trend here was caused by oils in the coffee, but the differences in contact angle were not pronounced enough to provide useful data with this method.

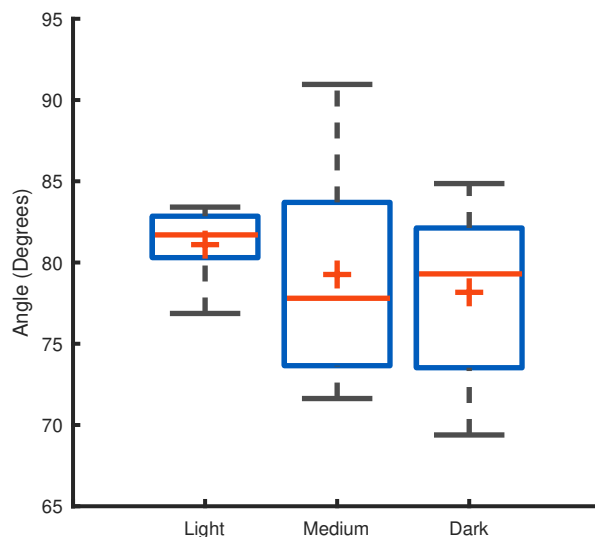


Figure F.2: Contact angle on Rain-X® coated slides on an aluminum block heated to 70 °C with the brewed coffee kept in a boiling water bath.

Repeating the test above on Indium Tin Oxide coated slides (a less hydrophobic surface) resulted in an upward trend again, but still not a significant difference.

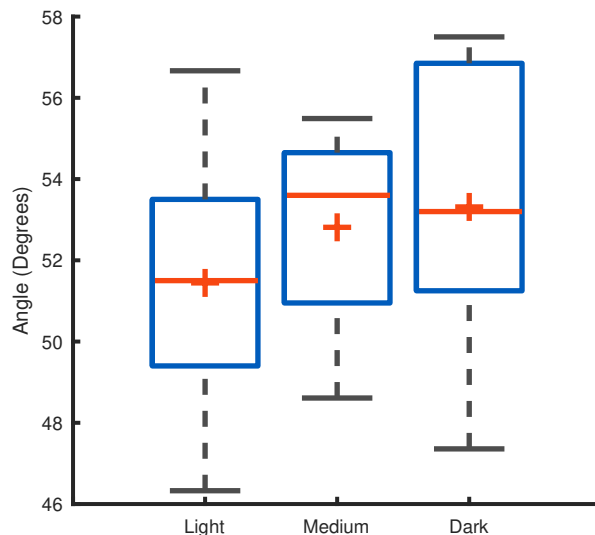


Figure F.3: Contact angle on InSnO coated slides on an aluminum block heated to 70 °C with the brewed coffee kept in a boiling water bath.

Changing the slide heating to human body temperature and using unheated slides (Figure F.4) reproduced the sudden cooling which occurs when drinking coffee. The hypothesis was that this could cause oils to precipitate out and change the surface tension. These tests did not show any significant difference between roast levels.

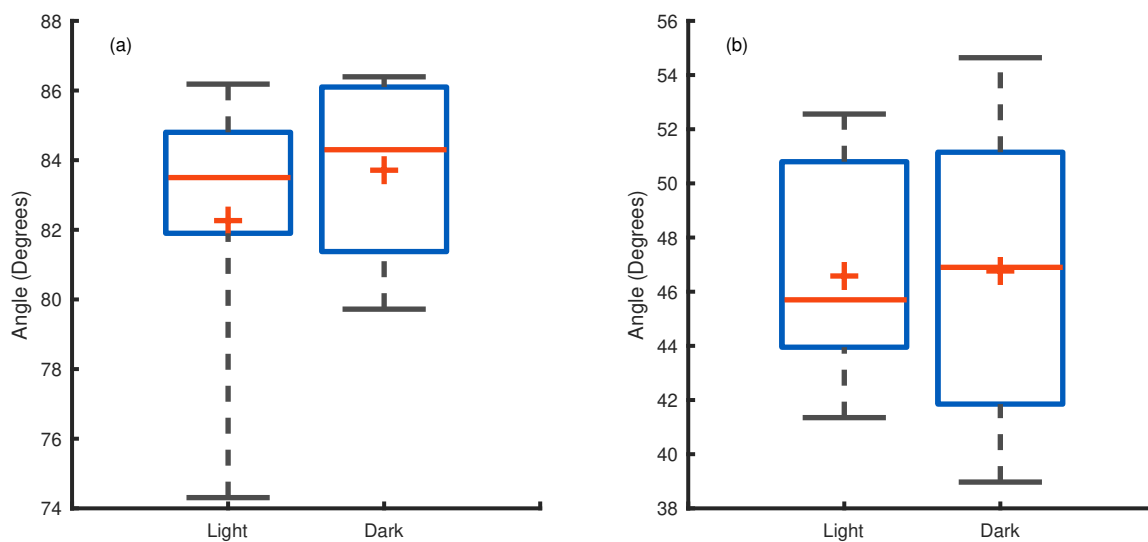


Figure F.4: Rain-X® coated slides heated to 37 °C (a) and InSnO coated slides without heating (b). In both cases, the coffee was in a boiling water bath until removed for sampling.

F.2 Viscosity

Body in coffee is sometimes used interchangeably with the term viscosity, as the mouth-feel of coffees with more body can give the impression of being thicker. Measuring the viscosity of unfiltered brewed coffee in a 75 °C water bath at different roast degrees did not show a significant difference in viscosity between light and dark roasts (Table F.1). Kinematic viscosity measurements came from a size 25 Cannon-Fenske viscometer, and specific gravity measured by weighing cooled coffee in a 50 mL volumetric flask allowed the dynamic viscosity to be calculated. Between each measurement, the viscometer was cleaned with ethanol and water. The viscosity of water measured before and after measuring the coffee viscosity demonstrated no issues with fouling.

Table F.1: Coffee viscosity results

	Time (s)	Kinematic Viscosity (cSt)	Specific Gravity	Dynamic Viscosity (cP)
Water	218.3	0.437	1	0.448
Light Roast	235.5	0.471	1.0064	0.480
Medium Roast	235.0	0.470	1.0064	0.479
Dark Roast	232.5	0.465	1.0064	0.474
Water	218.0	0.436	1	0.447

APPENDIX G Predicting Acidity with PLS Regression

Online acidity measurements with NIR were demonstrated in an existing study [52], so the main interest here was to determine whether the online acidity measurements are able to differentiate between roasts to the same roast degree with different temperatures and times, as used in the acidity control roasts (Section 3.4.6). The acidity PLS model used 60% of the roast degree dataset (Appendix A) and 84% of the acidity control data (Appendix E) for calibration and the remainder as the test dataset. The resulting model (Figure G.1) had an R^2 of 0.90.

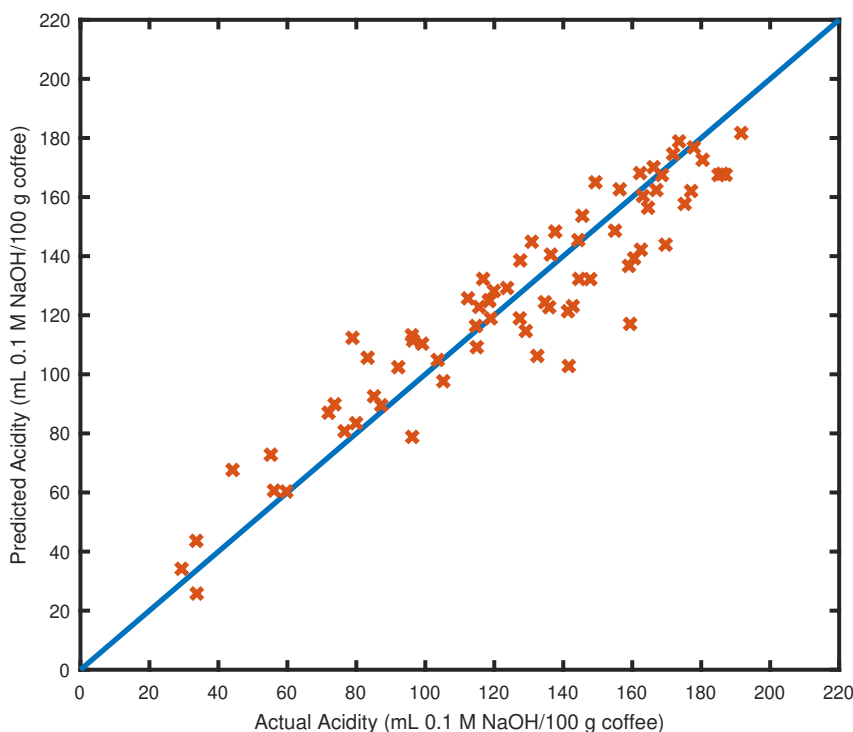


Figure G.1: Plot of acidity predictions vs measured values.

To see whether the model predicts acidity changes due to different roast temperatures at the same roast degree, the acidity control results which were not in the calibration dataset are shown in Figure G.2. The lines connect two sets of roasts to the same roast degree with the same coffee variety. Although there is some noise in

the results, there does appear to be an upward trend in the predictions which follows the actual acidity.

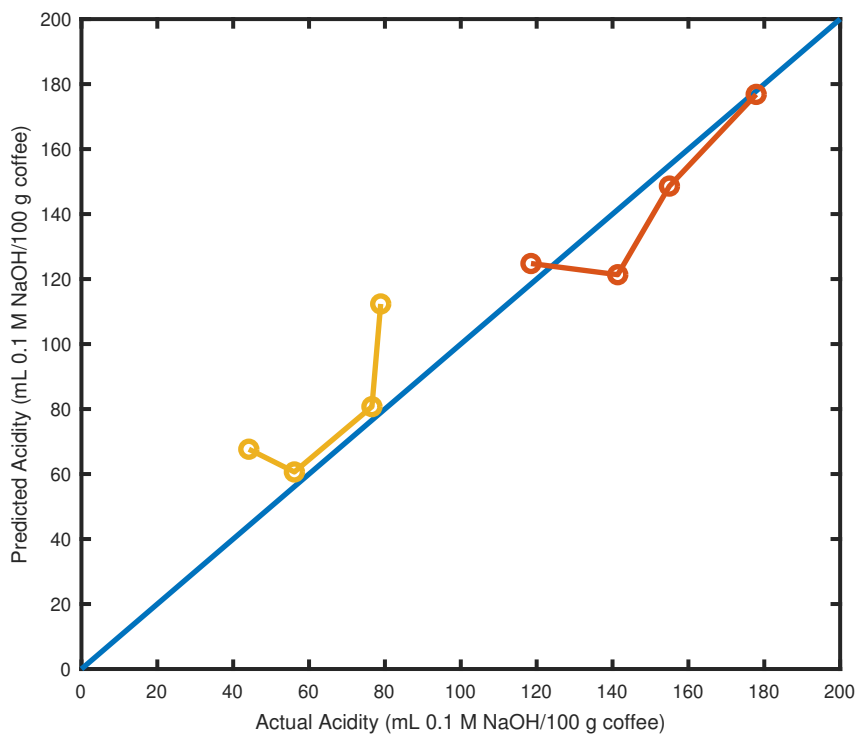


Figure G.2: Plot of acidity predictions vs measured values for a set of roasts to the same final roast degree with different roast profiles.

APPENDIX H Full Range NIR Spectrum

Figure H.1 shows the behavior of the full NIR spectrum of coffee from 900 to 2600 nm generated with two different spectrometers. The low wavelength spectrometer was a CDI NIR256L-1.7T1 grating spectrometer (Control Development Inc., South Bend, IN) with a range of 900-1700 nm, and the high wavelength spectrometer was a Si-Ware NeoSpectra SWS62221-2.5 Fourier transform NIR spectrometer (Si-Ware Systems, Egypt) with a range of 1300-2600 nm. The two sets of spectra came from two different roasts, because only one spectrometer could be used at a time, but the roasting parameters (coffee variety and quantity, temperature, and fan power) were identical in both roasts.

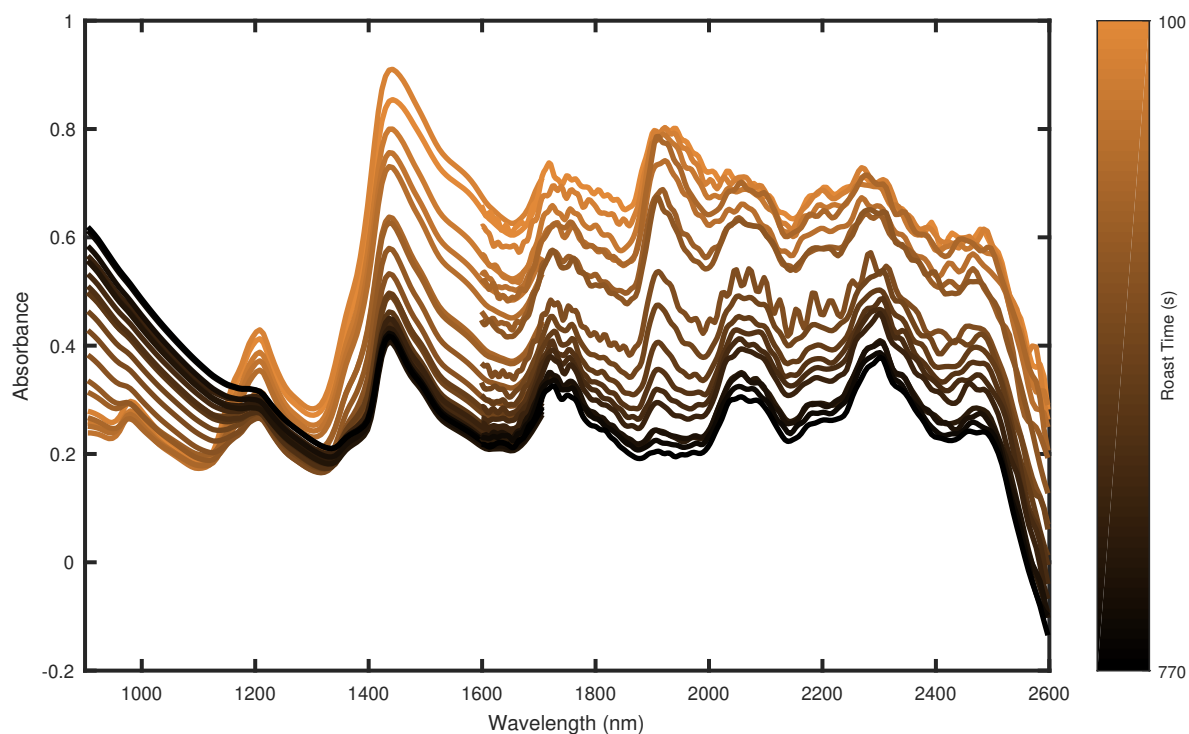


Figure H.1: Combined online NIR data from two NIR spectrometers with different wavelength ranges measured on two identical roasts.

This serves two purposes. First, it shows the full behavior of the coffee NIR spec-

trum, which increases in absorbance with roasting on the left side, similar to the visible spectrum, and decreases in absorbance on the right side. The transition from increasing to decreasing appears to occur between 1100 and 1300 nm, where the absorbance decreases initially and then increases. The drop in absorbance on the far right is caused by the reduced sensitivity of the spectrometer at those wavelengths. The second purpose of comparing the two spectrometers is to verify the accuracy of the Fourier transform spectrometer calibration. The overlapping regions of the spectrometer show the same peaks, which indicates that the wavelengths reported are accurate. Standard grating spectrometers do not require calibration, which allows the CDI spectrometer to be used as a reference.

APPENDIX I Online NIR Validation

Some aspects of the *in situ* NIR setup used in this study are uncommon in NIR spectroscopy and warrant validation. First, the NIR spectra were acquired through the glass roasting chamber, and second, the spectra were taken at non-constant temperatures, starting at room temperatures and reaching maximum temperatures near 220 °C.

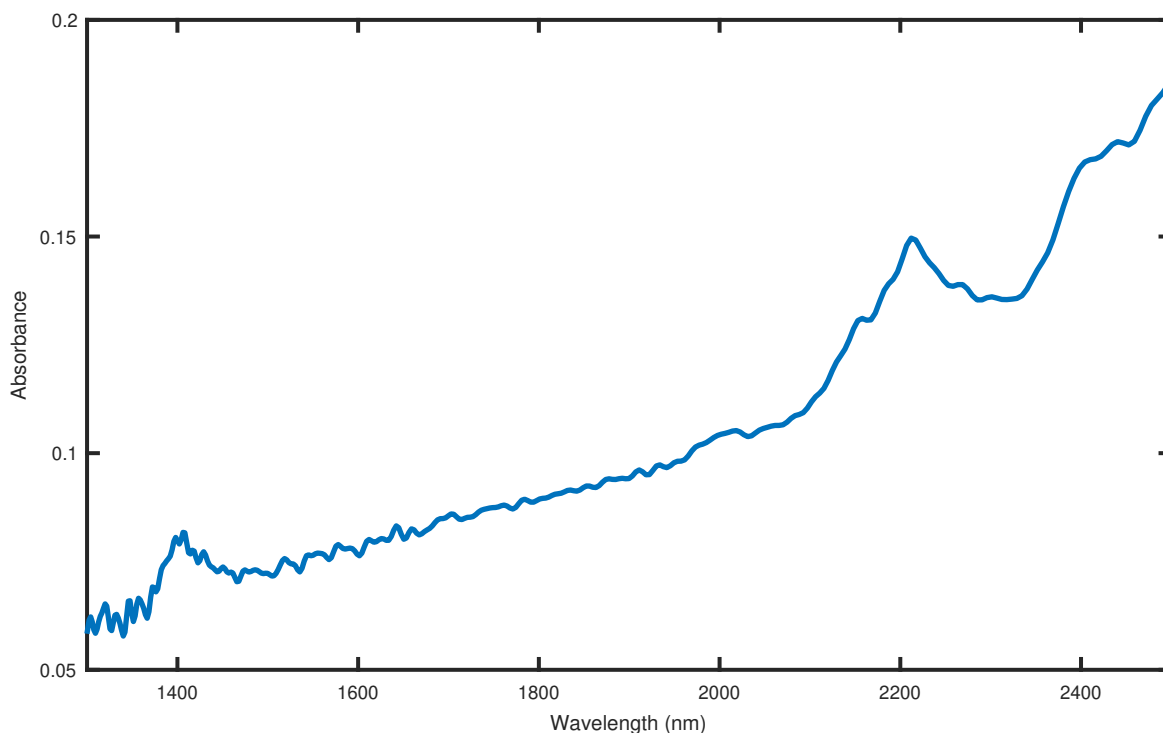


Figure I.1: NIR spectrum of the glass roasting chamber with a Teflon block inside, after subtracting the spectrum of the Teflon block without the roasting chamber as a reference.

The effect of the glass roasting chamber can be evaluated by measuring the reflectance of a Teflon block with and without the glass roasting chamber in place. The spectrum of the Teflon placed directly on the roaster without the glass roasting chamber was used as the 100% reflectance reference, and then the spectrum of the Teflon block with the roasting chamber in place was measured (Figure I.1). This shows the

absorbance of light by the glass. Some absorbance by the glass can be observed, but the main concern here was that the glass was not absorbing all of the light that reaches it and some light is still reflected back from inside the roasting chamber. This is evident from the figure and from the fact that changes in the *in situ* NIR spectra could be seen throughout the roast in previous figures.

The effect of temperature on the glass roasting chamber was another concern. This could not be measured with the Teflon block in place, because the roaster could not be run with the Teflon inside blocking airflow. Instead the spectrum of the empty glass roasting chamber at room temperature and at 230 °C (Figure I.2) provided an indication of whether a major change in reflection or emission by the glass occurs. Very little change in the NIR spectra can be seen between the two temperatures.

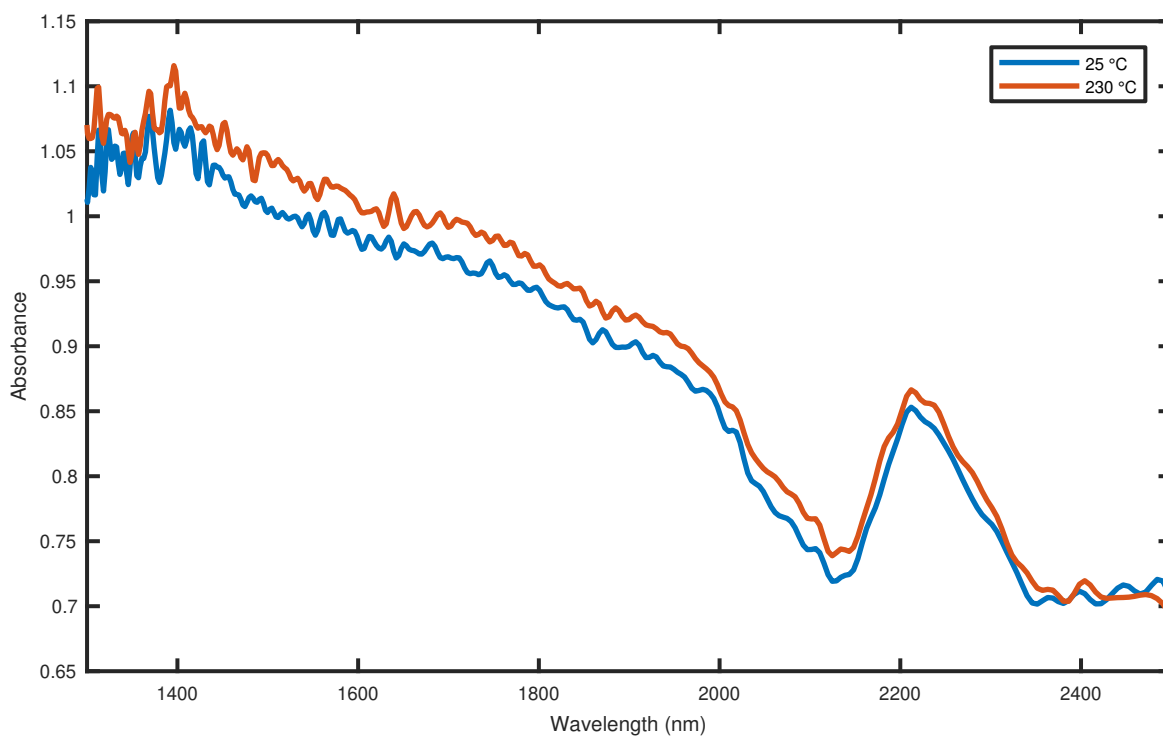


Figure I.2: NIR spectra of the empty glass roasting chamber at room temperature and at 230 °C.

APPENDIX J Crack Roast Degree Example

Figure J.1 shows an example plot of NIR darkness roast degree vs time during a roast. In this example, first crack occurs from NIR darkness values of 0.14 to 0.10 and second crack occurs from 0.04 to -0.02. The red dot represents time during the roast when the sample calculation takes place, which has an NIR darkness value of 0.07. The PLS models are applied to the NIR spectrum at this time, returning the predicted NIR darkness offset from each event, which would be -0.07, -0.03, 0.03, and 0.09 for first crack start, first crack end, second crack start, and second crack end respectively, assuming no prediction error.

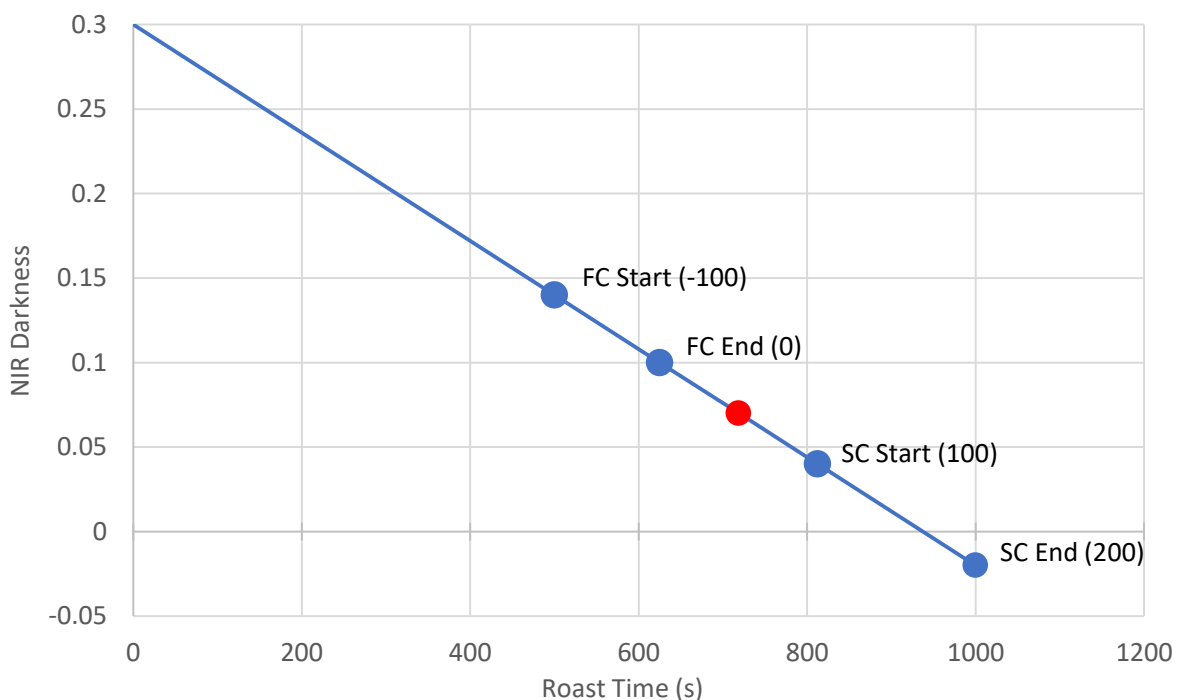


Figure J.1: Sample calculation of roast degree from crack predictions based on NIR darkness offset.

Based on the model output, the current time could be identified as between first and second crack, so its crack roast degree value should be between 0 and 100 based on

the reference values defined previously (Section 2.4.4). The exact roast degree value is then found by interpolation between 0 and 100 based on the NIR darkness offset values of the two nearest events (-0.03 and 0.03). Since the roast is directly between the two events, it has a crack roast degree of 50.